

Robust Pricing of Derivatives on Realised Variance



Gustav Ekman

University of Oxford

A thesis submitted for the degree of
Master of Science

Trinity 2019

Acknowledgements

I want to thank my supervisor for guiding me in my work on this dissertation, and I am grateful for his support on my journey through this fascinating topic.

Abstract

We investigate and compare the approaches of Carr & Lee [7] and Cox & Wang [12, 13] (the latter based on Root and Rost embeddings) for finding robust, model-independent bounds on the no-arbitrage prices of variance calls, and the associated sub- and superhedging strategies. The approaches are first compared from a theoretical viewpoint, and a correspondence between the subhedging strategies, based on a remark in Cox & Wang [13], is explicitly characterised. Next, the approaches are numerically implemented and tested on Black-Scholes and Heston models, and the obtained price bounds are compared and discussed. We find that for the models we implement, the Carr & Lee lower bounds are very close to the corresponding Root bounds, and that finding the Cox & Wang upper bound requires careful handling of the asymptotics of the Rost barrier.

Contents

1	Introduction	1
1.1	Project motivation	1
1.2	Project aim	2
1.3	Report outline	2
2	Theoretical background	3
2.1	Notation used	3
2.2	Traditional models	3
2.3	Variance swaps and options	4
2.4	Skorokhod embedding problem	6
2.5	Barriers and hitting times	7
2.6	Sub- and superhedging strategies	10
3	Two approaches for bounds	11
3.1	The Carr & Lee approach	11
(a)	Subhedging strategy	11
(b)	Superhedging strategy	14
3.2	The Cox & Wang approach	15
(a)	Root embedding and subhedging	15
(b)	Rost embedding and superhedging	17
3.3	Comparing the approaches theoretically	18
(a)	General observations	18
(b)	Carr & Lee subhedge as a special case of Root embedding	20
4	Numerical investigation	24
4.1	Simulating data	24
(a)	Path simulation	24
(b)	Determining distributions	25
(c)	Computing European call option prices	25
4.2	Carr & Lee method	26
(a)	Strategy of implementation	26
(b)	Numerical results	27
4.3	Cox & Wang method	29

(a)	Implementation of Root embedding	30
(b)	Implementation of Rost embedding	31
(c)	Numerical results	33
4.4	Comparison of numerical results	35
5	Conclusions	40
	Bibliography	41

List of Figures

2.1	Examples of (a) a Root barrier, and (b) a Rost barrier (grey regions). The stochastic process (blue) hits the barriers at the red marker.	8
4.1	Bounds on the no-arbitrage price for the Black-Scholes variance call. The lower bounds from Carr & Lee (“C & L”) and Cox & Wang (“C & W”) coincide with the true price. The upper bound “BB 1” is when we use the BB construction from the first time step, and “BB 2” from the second timestep.	28
4.2	Bounds on the no-arbitrage price for the Heston variance call. The lower bounds from Carr & Lee (“C & L”) and Cox & Wang (“C & W”) almost coincide. The upper bound “BB 1” is when we use the BB construction from the first time step, and “BB 2” from the second timestep.	29
4.3	Dimensionless implied volatilities for (a) the Black-Scholes data, and (b) the Heston data.	29
4.4	Root embedding for the data from the Black-Scholes model.	34
4.5	Root embedding for the data from the Heston model.	35
4.6	Rost embedding results for the data from the BS model for different uses of our Brownian bridge construction (BB).	36
4.7	Rost embedding results for the data from the Heston model for different uses of our Brownian bridge construction (BB).	37

Chapter 1. Introduction

1.1 Project motivation

Derivatives on the realised variance $\langle \log S \rangle_T$ of the price process S of an underlying asset have become increasingly common instruments for limiting volatility risk [7], and an important question is how to price and hedge such derivatives.

The traditional approach to derivatives pricing relies on the postulation of a stochastic model for the price process S of the underlying asset, imposing some dynamics for S under a risk-neutral pricing measure \mathbb{Q} . The time- t price V_t of an option is then given by the expression

$$V_t = \mathbb{E}_t^{\mathbb{Q}}[D_{t,T}F_T], \quad (1.1)$$

where F_T is a (generally path-dependent) functional of $(S_t)_{0 \leq t \leq T}$, and $D_{t,T}$ is the discount factor from time T to t [32]. Standard *vanilla European options* are written on the terminal value of an underlying asset, S_T . For example, the payoff of a European call option with strike price K and maturity T is given by

$$F(S_T) = (S_T - K)^+. \quad (1.2)$$

These derivatives are well-established and liquidly traded on the market, and their prices are determined by the principle of supply and demand. The question of derivative pricing is primarily concerned with the less liquidly traded *exotic derivatives* [32].

Oblój [44] presents three points of criticism against the traditional approach explained above: (i) the models only incorporate information such as prices of liquidly traded options through the act of calibration, and the models need to be frequently recalibrated; (ii) strong assumptions are made about e.g. the dynamics of the prices process; and (iii) the models fail to incorporate real world effects such as transactions costs and counterparty risk. Moreover, for models of the above types calibrated to the same market data, different models may yield different prices for the same exotic derivative [32].

An alternative approach to the classic one is to find robust and model-independent bounds on the no-arbitrage prices of derivatives. This robust approach eliminates, or at least minimises, model risk by imposing only weak modelling assumptions. In situations where the price of an exotic derivative might not be uniquely determined from the market data, the robust pricing methods allow us to at least bound the range of no-arbitrage prices, and the size of the no-arbitrage price range for an exotic derivative can provide some insight into the model risk associated with traditional pricing of it [7].

1.2 Project aim

The aim of this project is to investigate and compare the robust approaches found in Carr-Lee [7] and Cox-Wang [12, 13] for determining upper and lower bounds on the no-arbitrage price of options on realised variance. This will be done through both theoretical and numerical investigations of the two approaches.

1.3 Report outline

In Chapter 2 we provide a theoretical background and introduce relevant concepts and ideas. Next, in Chapter 3 we present specifically the approaches found in Carr & Lee [7] and Cox & Wang [12, 13] respectively, both of which are our main area of interest. After that, in Chapter 4, we numerically implement the methods and strategies from Carr & Lee and Cox & Wang, and compare the performance of these. Finally, in Chapter 5 we present the conclusions that we draw from our findings.

Chapter 2. Theoretical background

2.1 Notation used

We let S_t denote the time- t value of the price process of the underlying asset for $t \geq 0$. The notation $\langle \cdot \rangle$ is used for quadratic variation processes, and $x^+ := \max(x, 0)$. Pricing is done using the expectation under a pricing measure \mathbb{Q} as $\mathbb{E}_t^{\mathbb{Q}}[\cdot] := \mathbb{E}^{\mathbb{Q}}[\cdot | \mathcal{F}_t]$, where \mathcal{F}_t is the time- t filtration, and we will generally just write \mathbb{E}_t instead of $\mathbb{E}_t^{\mathbb{Q}}$ when it is clear from the context what measure is used, with $\mathbb{E}_0 = \mathbb{E}$ being the unconditional expectation. Unless otherwise specified, W is a standard Brownian motion, and Z a geometric Brownian motion. ν will be used for the initial (time-0) distribution of a stochastic process, and μ denotes the distribution of the process at some future time (usually the maturity of an option). $\text{supp}(\chi)$ is the support of the distribution χ , and $\mathcal{L}(X)$ is the law of the random variable X . $\mathcal{U}([a, b])$ is the uniform distribution on the interval $[a, b]$, $\mathcal{N}(\mu, \sigma^2)$ the normal distribution with mean μ and variance σ^2 , and $\delta_a(x) := \delta(x - a)$ is the Dirac delta function. $C_t(K)$ and $P_t(K)$ are the time- t values of European calls and puts on S_T with strike K . For any domain \mathcal{A} , $\mathcal{C}(\mathcal{A})$ is the class of functions that are continuous on \mathcal{A} .

2.2 Traditional models

One of the fundamental classical models for derivatives pricing is that of Black-Scholes [2], which Merton [39] contributed to. In the Black-Scholes model, the dynamics of the price process are given by

$$\frac{dS_t}{S_t} = rdt + \sigma dW_t, \quad (2.1)$$

where r is the (constant) interest rate, σ the (constant) volatility, and W_t a \mathbb{Q} -Brownian motion. While this model is useful for its simplicity and tractability, it fails to capture many observed real-world phenomena, such as transaction costs, non-constant interest rates and volatilities, limitations on the liquidity etc. [51]. There are several extensions to this model that allow for a richer description of the asset dynamics by e.g. allowing for non-constant parameters in the stochastic differential equation (SDE) (2.1). These include various forms of local volatility [15, 20, 25], stochastic volatility [31, 34, 49], and stochastic-local volatility models [30, 36, 52]. An example of such an extension is the stochastic volatility model introduced by Heston [31], in which the variance v_t follows a Cox-Ingersoll-Ross process [14],

and the price process S has the risk-neutral dynamics

$$\begin{aligned} dS_t &= rS_t dt + \sqrt{v_t} S_t dW_t, \\ dv_t &= \kappa[\theta - v_t] dt + \varsigma \sqrt{v_t} d\widehat{W}_t, \end{aligned} \tag{2.2}$$

where r is a (constant) interest rate, $\kappa > 0$ governs the speed of reversion to level $\theta > 0$, and $\varsigma > 0$ is the volatility of the variance process v_t , which has initial value $v_0 > 0$. If the Feller condition $2\kappa\theta > \varsigma^2$ is satisfied, then the variance process will always stay positive [1]. The two Brownian motions W and \widehat{W} have correlation ρ .

2.3 Variance swaps and options

Consider an asset with dynamics

$$\frac{dS_t}{S_t} = r_t dt + \sigma_t dW_t, \tag{2.3}$$

where r_t is a deterministic interest rate process, and $\sigma_t > 0$ is some volatility process, which in general is stochastic (it could also be a deterministic process, and even a constant as in the Black-Scholes model). Then the *realised variance* of the price process S at time T is given by the expression

$$\int_0^T \sigma_t^2 dt = \int_0^T \frac{d\langle S \rangle_t}{S_t^2} = \langle \log S \rangle_T. \tag{2.4}$$

Hence, the payoffs of derivatives on realised variance can be expressed as $F(\langle \log S \rangle_T)$ or, if we define $X := \log S$, as $F(\langle X \rangle_T)$, for some payoff function F . In order to simplify the notation in our later arguments, we will make the assumption of zero interest rates in (2.3) for the remainder of this report. This does not result in any loss of generality compared to the case with arbitrary deterministic interest rates, since deterministic interest rates do not impact the quadratic variation [7]. To see this, consider a modified price process with dynamics $d\tilde{S}/\tilde{S} = \sigma_t dW_t$. We have

$$\log S_T = \log S_0 + \int_0^T r_t dt + \int_0^T \sigma_t dW_t - \int_0^T \frac{\sigma_t^2}{S_t^2} dt, \tag{2.5}$$

and thus

$$\langle \log \tilde{S} \rangle_T = \int_0^T \sigma_t^2 dt = \langle \log S \rangle_T, \tag{2.6}$$

so the two processes have the same realised variance. Moreover, under the assumption $r = 0$, the prices of derivatives will be given by their expected payoffs without the need to discount. Note that stochastic interest rates, on the other hand, could indeed affect the quadratic variation of the price process, so some of the results presented here will only extend to settings with deterministic rates.

In reality, contracts are usually not written on the continuous time realised variance as specified in (2.4), but rather on a discretised version thereof [9, 12], often of the form [6, 17]

$$RV_T = \sum_{i=1}^N \left(\log \frac{S_{t_i}}{S_{t_{i-1}}} \right)^2, \tag{2.7}$$

for some sequence of times t_i with $t_i = 0$ and $t_N = T$, usually using a daily frequency. For studies on the deviations between the continuous and discrete time definitions of realised variance, see e.g. Bondarenko [3], Jarrow et al. [35], and Hobson & Klimmek [33].

For the simple case of a so-called *variance swap*, we have the payoff

$$F(\langle X \rangle_T) = \langle X \rangle_T - Q, \quad (2.8)$$

for some constant Q . Using Itô's lemma on the process $\log(S_T)$, we obtain

$$\log(S_T) = \log(S_0) + \int_0^T \frac{1}{S_t} dS_t - \frac{1}{2} \langle X \rangle_T \quad (2.9)$$

or rearranged

$$\langle X \rangle_T = -2 \log(S_T/S_0) + 2 \int_0^T \frac{1}{S_t} dS_t. \quad (2.10)$$

Hence, as shown by Dupire [24] and Neuberger [42], we can perfectly replicate the realised variance $\langle X \rangle_T$ by employing a trading strategy consisting of a claim on a log-contract with payoff $-2 \log S_T/S_0$, and self-financing continuous trading so that we are long $2/S_t$ shares [9]. Using integration by parts twice (see e.g. Appendix 1 in [8]), any twice differentiable function $F(x)$ may be written in the form

$$\begin{aligned} F(x) = & F(x_0) + F'(x_0)[(x - x_0)^+ - (x_0 - x)^+] \\ & + \int_0^{x_0} F''(K)(K - x)^+ dK + \int_{S_0}^{\infty} F''(K)(x - K)^+ dK, \end{aligned} \quad (2.11)$$

for some constant $x_0 \geq 0$. Then, under the assumption that European put and call options with maturity T are available at all strikes K , the log-contract can be perfectly replicated using the following decomposition (see also Demeterfi [19])

$$\log \frac{S_T}{S_0} = \frac{S_T - S_0}{S_0} - \int_0^{S_0} \frac{1}{K^2} (K - S_T)^+ dK - \int_{S_0}^{\infty} \frac{1}{K^2} (S_T - K)^+ dK. \quad (2.12)$$

Thus, we are able to replicate variance swaps using bonds, stocks, and vanilla European options. In particular, using (2.10) and (2.12), the price of the realised variance will be given by (recall that we price using expectation)

$$\mathbb{E}_t \langle X \rangle_T = -2 \mathbb{E}_t \log \frac{S_T}{S_0} = -2 \frac{S_t - S_0}{S_0} + 2 \int_0^{S_0} \frac{1}{K^2} P_t(K) dK + 2 \int_{S_0}^{\infty} \frac{1}{K^2} C_t(K) dK. \quad (2.13)$$

In addition, there are *variance options*, which are options on the realised variance of the process S . An example is the (*spot-starting*) *variance call* with payoff

$$(\langle X \rangle_T - Q)^+ = \left(\int_0^T \frac{d\langle S \rangle_t}{S_t^2} - Q \right)^+ = \left(\int_0^T \sigma_t^2 dt - Q \right)^+. \quad (2.14)$$

Such derivatives prove to be more challenging to price, as the choice of model will affect what price the variance option is assigned. There are also *forward-starting* variance calls with payoff $(\langle X \rangle_T - \langle X \rangle_\theta)^+$ for some $\theta \in [0, T)$.

Although we frequently use the term “variance options”, we mainly consider the pricing of variance calls. Since we are able to robustly replicate the variance swap $\langle X \rangle_T - Q$ using

(2.10), once we have obtained price bounds for the call options we can easily find bounds for the put options by using the put-call parity for the payoffs

$$(Q - \langle X \rangle_T)^+ = (\langle X \rangle_T - Q)^+ + Q - \langle X \rangle_T. \quad (2.15)$$

Hence, there is no loss of generality in focusing on the case of call options.

Now, let μ be the distribution of the underlying at maturity, i.e. $S_T \sim \mu$. Using the Breeden-Litzenberger [4] formula (assuming C_t is twice differentiable)

$$\mu(dK) = \frac{\partial^2}{\partial K^2} C_t(K) dK, \quad (2.16)$$

the distribution μ can be recovered from the call prices observed in the market. We then consider all models under which the price process is a martingale with distribution μ at maturity: the family of *admissible models* that are consistent with the market data. To robustly bound the no-arbitrage price, we need to determine the range of prices that these models produce, and in particular the minimal and maximal prices.

2.4 Skorokhod embedding problem

One of the challenges of robust pricing is to determine the extremal prices from the family of admissible models, and to characterise the associated martingale price processes. One approach is to relate the pricing problem to the Skorokhod embedding problem (SEP henceforth). The SEP, originally formulated and solved by Skorokhod [50], is defined as:

Definition 2.1. Skorokhod embedding problem. Given a stochastic process $Y = (Y_t)_{t \geq 0}$ and a measure μ , find a *minimal* stopping time τ such that the stopped process Y_τ has $\mathcal{L}(Y_\tau) = \mu$.

Minimal in Definition 2.1 means that for every stopping time $\rho \leq \tau$ such that $Y_\rho \sim \mu$ we have $\rho = \tau$ almost surely [32]. Solutions to the SEP above are said to *embed* μ in Y , and we denote by $SEP(Y, \mu)$ the set of solutions to the SEP that embed the distribution μ in the process Y . In general, the process Y may have any initial distribution $Y_0 \sim \nu$, with $Y_0 \sim \delta_0$ being a special case. By Monroe [40] we have:

Proposition 2.2. (Monroe [40]) For any stopping time τ there is a minimal stopping time $\theta \leq \tau$ such that $\mathcal{L}(W_\theta) = \mathcal{L}(W_\tau)$.

By the results of Dambis [16] and Dubins & Schwarz [23], every continuous local martingale M is equivalent to a time-changed Brownian motion $M_t = W_{\langle M \rangle_t}$. Specifically, for the local martingale $M_t = \int_0^t dS_t/S_t$ we have $\langle M \rangle_t = \langle X \rangle_t$, and we may thus write [7, 32]

$$M_t = W_{\langle M \rangle_t} = W_{\langle X \rangle_t}. \quad (2.17)$$

Furthermore, from (2.9) we have the dynamics

$$X_t = X_0 + M_t - \frac{1}{2} \langle X \rangle_t, \quad (2.18)$$

and hence, combined with (2.17), we obtain

$$S_t = \exp(X_t) = \exp\left(X_0 + M_t - \frac{1}{2}\langle X \rangle_t\right) = S_0 \exp\left(W_{\langle X \rangle_t} - \frac{1}{2}\langle X \rangle_t\right) = Z_{\langle X \rangle_t}, \quad (2.19)$$

where Z_t is the (martingale) geometric Brownian motion given by

$$Z_t = S_0 \exp\left(W_t - \frac{1}{2}t\right). \quad (2.20)$$

We then have $Z_{\langle X \rangle_T} = S_T \sim \mu$, and so $\langle X \rangle_T$ embeds the distribution μ in the process Z , i.e. $\langle X \rangle_T \in SEP(Z, \mu)$. Similarly, for each stopping time $\tau \in SEP(Z, \mu)$, we can find an associated continuous martingale process through the construction

$$\tilde{S}_t = Z_{\tau \wedge \frac{t}{T-t}}. \quad (2.21)$$

This martingale process satisfies both $\tilde{S}_0 = S_0$ and $\tilde{S}_T = Z_\tau \sim \mu$. Moreover, the payoff of a variance call for this martingale process is

$$(\langle \log \tilde{S} \rangle_T - Q)^+ = (\langle \log Z \rangle_\tau - Q)^+ = (\langle W \rangle_\tau - Q)^+ = (\tau - Q)^+. \quad (2.22)$$

We find that every solution $\tau \in SEP(Z, \mu)$ will be equivalent to some possible martingale price process \tilde{S} for the underlying, and thus correspond to some expected payoff and price for the variance call. Hence, we can characterise the admissible models in terms of their associated stopping times, and bound the no-arbitrage price by solving

$$\inf_{\tau \in SEP(Z, \mu)} \mathbb{E}(\tau - Q)^+ \quad \text{and} \quad \sup_{\tau \in SEP(Z, \mu)} \mathbb{E}(\tau - Q)^+, \quad (2.23)$$

for the lower and upper bounds respectively [32].

2.5 Barriers and hitting times

Consider the problem of finding a minimal stopping time τ_R that yields a lower bound on the price, i.e. a stopping time that minimises $\mathbb{E}[(\tau - Q)^+]$. Such a stopping time was first described by Root [46], its optimality proven by Rost [48], and it is one of the main focuses of this section. We first need to introduce the concept of a *barrier*, as in Definition 2.3 below.

Definition 2.3. (Root [46]) A *barrier* (or *Root barrier*) is a subset \mathcal{B} of $[0, +\infty] \times [-\infty, +\infty]$ satisfying

1. \mathcal{B} is closed,
2. $(+\infty, x) \in \mathcal{B}$ for all $x \in [-\infty, +\infty]$,
3. $(t, \pm\infty) \in \mathcal{B}$ for all $t \in [0, +\infty]$,
4. if $(t, x) \in \mathcal{B}$ then $(s, x) \in \mathcal{B}$ whenever $s > t$.

We may then formally define the hitting time (see e.g. Protter [45]) $\tau_{\mathcal{B}}$ of a barrier \mathcal{B} for a stochastic process Y as $\tau_{\mathcal{B}} = \inf\{t > 0 : (t, Y_t) \in \mathcal{B}\}$, and we will call such a hitting time a *Root stopping time*, or a *Root embedding* if the hitting time is a solution to the SEP. See Figure 2.1a for an example of a Root barrier.

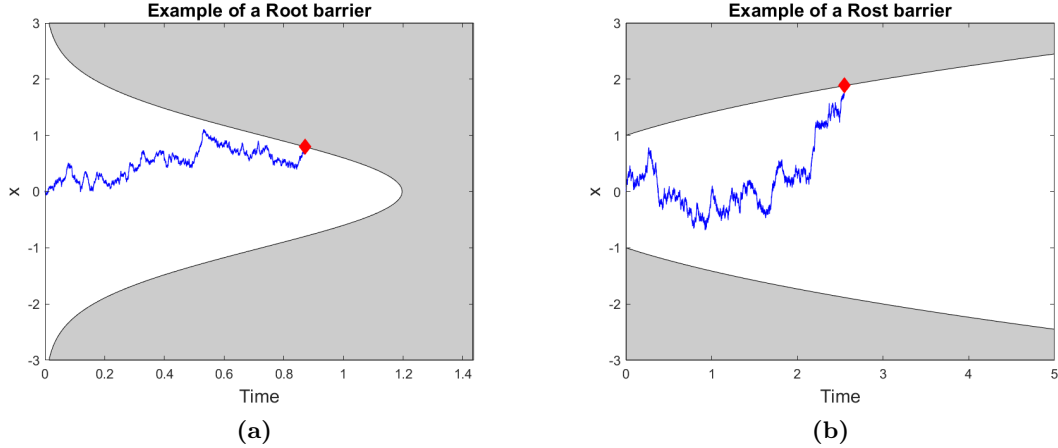


Figure 2.1: Examples of (a) a Root barrier, and (b) a Rost barrier (grey regions). The stochastic process (blue) hits the barriers at the red marker.

As shown by Monroe [40], all hitting times are minimal, and all stopping times with finite expectation are minimal. Thus, embeddings defined through barriers will give minimal solutions to the SEP. Furthermore, by Loynes [38], every barrier \mathcal{B} can be expressed in the form $\mathcal{B} = \{(x, t) : t \geq R(x)\}$ for some lower semi-continuous *barrier function* $R : \mathbb{R} \rightarrow [0, \infty]$, and the Root barrier is unique (see Theorem 1 in Loynes [38]).

A relevant concept for our purposes is that of *minimal residual expectation*, see Definition 2.4. It was first introduced by Dinges [21] for the discrete time case, and generalised to continuous time by Rost [48] (here we use the definition from Cox & Wang [13]).

Definition 2.4. (Cox & Wang [13]) A stopping time $\tau^* \in SEP(Y, \mu)$ is said to be of *minimal residual expectation* (with respect to μ) if, for each $t \in \mathbb{R}_+$, it minimises the quantity

$$\mathbb{E}(\tau - t)^+ = \mathbb{E} \int_{\tau \wedge t}^{\tau} ds = \int_t^{\infty} \mathbb{P}(\tau > s) ds, \quad (2.24)$$

over all $\tau \in SEP(Y, \mu)$.

Furthermore, any convex function F can be written in terms of positively weighted functions of the form $(x - K)^+$ [13, 32], and hence, as first shown by Dinges [21], any solution of minimal residual expectation also minimises the quantity $\mathbb{E}[F(\tau)]$ for all convex functions F .

With Definition 2.5 of the *potential* of a distribution, we also get Theorems 2.6 and 2.7, first shown by Rost [48]. We here use the definition of the potential from Cox & Wang [13], which differs from that of Rost [48] by a minus sign. Moreover, in contrast with Rost [48], we use ν for the initial distribution and μ for the target distribution.

Definition 2.5. (Cox & Wang [13]) The *potential* U_χ of a distribution χ is given by

$$U_\chi(x) := - \int_{\mathbb{R}} |y - x| \chi(dy). \quad (2.25)$$

Theorem 2.6. (Rost [48]) If a measure μ satisfies $U_\nu \geq U_\mu$, then there exists a stopping time of minimal residual expectation (with respect to μ).

Theorem 2.7. (Rost [48]) Every Root stopping time τ is of minimal residual expectation (with respect to μ).

Note that the condition $U_\nu \geq U_\mu$ in Theorem 2.6 implies that the distributions ν and μ have the same mean [10]. In addition, the corollary to Theorem 3 in Rost [48] says that for processes Y with regular one-point sets, any embedding with minimal residual expectation is also a Root stopping time. Hence, under appropriate assumptions on the target distribution μ and the process Y , we are ensured that a solution to the $SEP(Y, \mu)$ of minimal residual expectation can be obtained using Root barriers. Using the fact that if $\mathbb{E}[\tau] < \infty$ then $\mathbb{E}[\tau] = \int x^2 \mu(dx)$ for all embeddings τ [32], and that the Root time minimises $\mathbb{E}[F(\tau)]$ for F convex, the Root stopping time is the embedding with minimal variance $\mathbb{E}[(\tau - \mathbb{E}[\tau])^2]$.

Since the Root stopping time τ_R minimises the expectation $\mathbb{E}(\tau_R - Q)^+$, we may use it to obtain a lower bound on the price of a variance option with payoff $(\int_0^T \sigma_t^2 dt - Q)^+$. Nonetheless, the difficulty of finding an explicit characterisation of the Root barrier remains, and so any attempts to find price bounds using the Root embedding must overcome this challenge.

So far, we have outlined how to use the Root embedding to find a lower bound on the price of a variance call. In an analogous fashion, we will be able to use a *reverse barrier* $\bar{\mathcal{B}}$ (see Definition 2.8) to find upper price bounds. The corresponding stopping time was first introduced by Rost [47], and Chacon [10] showed how reversed barriers could be used to characterise these stopping times. Similarly to the Root barrier, the reverse barrier can be formulated in the form $\bar{\mathcal{B}} = \{(t, x) : t \leq \bar{R}(x)\}$ for some *reverse barrier function* $\bar{R} : \mathbb{R} \rightarrow \mathbb{R}_+$ [32]. See Figure 2.1b for an example of a reverse barrier.

Definition 2.8. (Obłój [43]) A *reverse barrier* (or *Rost barrier*) is a subset $\bar{\mathcal{B}}$ of $[0, +\infty) \times [-\infty, +\infty]$ satisfying

1. $\bar{\mathcal{B}}$ is closed,
2. $(0, x) \in \bar{\mathcal{B}}$ for all $x \in [-\infty, +\infty]$,
3. $(t, \pm\infty) \in \bar{\mathcal{B}}$ for all $t \in [0, +\infty]$,
4. if $(t, x) \in \bar{\mathcal{B}}$ then $(s, x) \in \bar{\mathcal{B}}$ whenever $s < t$.

By the results of Rost [47], if a hitting time $\tau_{\bar{\mathcal{B}}}$ of a reverse barrier $\bar{\mathcal{B}}$ solves the SEP, then it maximises the residual expectation $\mathbb{E}(\tau - t)^+$ for all $t \in \mathbb{R}_+$ [32, 43]. We will refer to the hitting time of a reverse barrier as a *Rost stopping time* or *Rost embedding*,

in analogy with the Root stopping times. Under the assumptions of Theorem 2.6 and the additional assumption that the initial distribution ν and the target distribution μ have disjoint support, we are ensured the existence of a reverse barrier \bar{B} such that its hitting time $\tau_{\bar{B}}$ is in $SEP(Z, \mu)$ (the case where the distributions are not disjoint can be handled using external randomisation) [12].

By similar arguments as for the Root times above, the Rost hitting time $\tau_{\bar{R}}$ is of finite expectation and maximises the quantity $\mathbb{E}[F(\tau)]$ for all non-negative convex functions F [12], hence also being the embedding of maximal variance. We may thus use Rost stopping times to find upper bounds on the no-arbitrage price of variance options.

Intuitively, we can think of the Root and Rost embeddings as extremal embeddings, where the Root barrier stops the process Z_t at a relatively narrow cluster of times (hence the low variance), and the Rost barrier stops the process more evenly spread out over time (resulting in a higher variance) [7, 27].

2.6 Sub- and superhedging strategies

An alternative approach to bounding the no-arbitrage price of variance options is to consider general *sub-/super-replicating* trading strategies, also known as *sub-/superhedging* strategies. A definition of these is given below:

Definition 2.9. A trading strategy $G(t)$ ($G(t) - G(0)$ being self-financing) is said to (robustly) *sub-replicate/subhedge* a derivative $F(t)$ if at all times $t \in [0, T]$ we have $G(t) \leq F(t)$ almost surely. Conversely, if we have $G(t) \geq F(t)$ almost surely for all $t \in [0, T]$, then the strategy $G(t)$ is said to be a (robust) *super-replicating/superhedging* strategy of $F(t)$.

By finding sub- and superhedging strategies $G_{\text{sub}}, G_{\text{super}}$ that satisfy the pathwise inequalities $G_{\text{sub}}(t) \leq F(t)$ and $G_{\text{super}}(t) \geq F(t)$ respectively, and using the assumed absence of arbitrage, we may bound the price of F by the prices of G_{sub} and G_{super} . To see how such strategies can be used to bound the price, assume that we have a subhedging portfolio $G(t) \leq F(t)$. Now, if F is priced lower than G , then go long F and short G to make an initial profit. At maturity $F - G \geq 0$ and so we will have made a risk-free profit, contradicting our assumption about the absence of arbitrage. The fact that superhedging portfolios give upper bounds on the price of F follows by similar arguments.

Using sub- and superhedging, we thus have an alternative approach for bounding the no-arbitrage price of the variance option. If we use strategies for which the inequalities $G_{\text{sub}}(t) \leq F(t)$ and $G_{\text{super}}(t) \geq F(t)$ hold on a pathwise basis, we obtain robust price bounds, since the inequalities do not depend on any particular model for the price process and are valid for all continuous paths.

Chapter 3. Two approaches for bounds

In this chapter, we focus on two different approaches for bounding the no-arbitrage price of variance call options: (i) the sub- and superhedging strategies of Carr & Lee [7]; and (ii) the approach by Cox & Wang [12,13] using the optimality and embedding properties of the Root and Rost hitting times. The approaches are explained in greater detail below.

3.1 The Carr & Lee approach

In [9], Carr & Lee assume that the price process S of the underlying with reinvested dividends is a positive continuous semimartingale on the filtered space $(\Omega, \mathcal{F}, \{\mathcal{F}_t\}, \mathbb{P})$, where \mathbb{P} is the physical probability measure. In this context, Carr & Lee are then able to derive sub- and superhedging strategies for variance calls, and by arguments similar to those presented in Section 2.6, they show that the strategies yield lower and upper bounds on the no-arbitrage price.

(a) Subhedging strategy

The subhedging strategy presented in this section is attributed to Dupire [26], and it was generalised by Carr & Lee to forward-starting options. The results for spot-starting variance calls are summarised in Proposition 3.1. Some comments on the functions used in the proposition are given below.

Proposition 3.1. (Dupire [26]) *Let $\lambda : \mathbb{R}_+ \rightarrow \mathbb{R}$ be a convex function with left-hand derivative λ_y , and its second derivative λ_{yy} satisfying*

$$\lambda_{yy} \leq 2/y^2, \quad \forall y \in \mathbb{R}_+ \tag{3.1}$$

in a distributional sense. In addition, let $\tau_Q := \inf\{t \geq 0 : \langle X \rangle_t = Q\}$, and define the functions

$$BS(y, v; f) := \begin{cases} \int_{-\infty}^{\infty} f(ye^z) \frac{1}{\sqrt{2\pi v}} \exp\left(-\frac{(z+v/2)^2}{2v}\right) dz & \text{if } v > 0, \\ f(y) & \text{if } v = 0, \end{cases} \tag{3.2}$$

and

$$N_t := \begin{cases} -BS_y(S_t, Q - \langle X \rangle_t; \lambda) & \text{if } t \leq \tau_Q, \\ -\lambda_y(S_t) & \text{if } t > \tau_Q. \end{cases} \tag{3.3}$$

Then for any λ satisfying the above assumptions, the strategy of holding at each time $t \in [0, T)$ the portfolio

$$\begin{cases} 1 \text{ claim on } \lambda(S_T), \\ N_t \text{ shares,} \\ -BS(S_0, Q; \lambda) + \int_0^t N_s dS_s - N_t S_t \text{ bonds,} \end{cases} \quad (3.4)$$

subhedges the payoff $((X)_T - Q)^+$, and its time-0 price $-BS(S_0, Q; \lambda) + \mathbb{E} \lambda(S_T)$ gives a lower bound on the no-arbitrage price of the variance call.

Furthermore, define

$$\text{van}_K(y) := \begin{cases} (y - K)^+ & \text{if } K \geq S_0, \\ (K - y)^+ & \text{if } K < S_0, \end{cases} \quad (3.5)$$

and for each strike K let $I_0(K, T)$ be the unique dimensionless implied volatility such that

$$BS(S_0, I_0(K, T); \text{van}_K) = \mathbb{E} \text{van}_K(S_T) \quad (3.6)$$

holds. Then out of all admissible λ , the choice

$$\lambda(y) = \int_{\{K: I_0(K, T) > Q\}} \frac{2}{K^2} \text{van}_K(y) dK \quad (3.7)$$

maximises the value of the lower bound.

Note that $\lambda(S_T)$ is a European claim on S_T , and that its price can be determined from the vanilla call prices $C_0(K)$ and put prices $P_0(K)$ over all strikes K , which are given by the market.

By trivially rewriting the function BS using the following change of variables

$$BS(y, v; f) = \int_{-\infty}^{\infty} f(ye^z) \frac{1}{\sqrt{2\pi v}} \exp\left[-\frac{(z + v/2)^2}{2v}\right] dz \quad (3.8)$$

$$= \int_0^{\infty} f(w) \frac{1}{w\sqrt{2\pi v}} \exp\left[-\frac{(\log(w/y) + v/2)^2}{2v}\right] dw, \quad (3.9)$$

we clearly see that, as stated in Carr & Lee [7], we can interpret the function $BS(y, v; f)$ as returning the Black-Scholes prices of a European contract with payoff function f , given that $S_0 = y$, $r = 0$, and $\sigma^2 T = v$, with the special case $BS(y, v; f) = f(y)$ if $v = 0$.

We will now briefly comment on why the function N_t in the subhedging strategy is divided into two distinct steps, summarising some of the arguments and observations in Carr & Lee [7]. The overarching idea is that for $t \leq \tau_Q$ we try to replicate a claim on $-\lambda(S_{\tau_Q})$ using $BS(y, v; f)$, and for $t > \tau_Q$ we dynamically trade to ensure subreplication of the variance call payoff. In particular, if $\tau_Q \leq T$, then using the strategy in Proposition 3.1 we will have replicated $-\lambda(S_{\tau_Q})$ by time τ_Q [7], and thus end up with a portfolio consisting of a claim on $\lambda(S_T)$ and a claim on $-\lambda(S_{\tau_Q})$. By dynamically trading until maturity T as specified above, the subhedging strategy will yield a payoff of

$$\begin{aligned} \lambda(S_T) - \lambda(S_{\tau_Q}) - \int_{\tau_Q}^T \lambda_y(S_t) dS_t &= \frac{1}{2} \int_{\tau_Q}^T \lambda_{yy}(S_t) d\langle S \rangle_t \\ &\leq \int_{\tau_Q}^T \frac{d\langle S \rangle_t}{S_t^2} = (\langle \log S \rangle_T - \langle \log S \rangle_{\tau_Q})^+ = ((X)_T - Q)^+, \end{aligned} \quad (3.10)$$

where the first equality follows from Itô's lemma, and the inequality is a result of the assumption $\lambda_{yy} \leq 2/y^2$. If on the other hand $\tau_Q > T$, we do not succeed in replicating $-\lambda(S_{\tau_Q})$ and instead end up at maturity with the payoff $-BS(S_T, Q - \langle X \rangle_T; \lambda) + BS(S_T, 0; \lambda) \leq 0 = (\langle X \rangle_T - Q)^+$, where the inequality holds by the fact that BS is increasing in Q for convex λ (since Vega is positive for convex European payoffs). In either case, we will always subreplicate the variance call, and so the strategy subreplicates almost surely.

Now let us direct our attention to the question of selecting a suitable function λ for the subhedging strategy. First consider the choice

$$\lambda(y) = -2 \log(y/S_0) + 2S_0^{-1}(y - S_0). \quad (3.11)$$

This choice clearly satisfies the conditions of Proposition 3.1 (note that $\lambda_{yy} = 2/y^2$), and using (2.11) we may rewrite λ as

$$\lambda(y) = \int_0^\infty \frac{2}{K^2} \text{van}_K(y) dK. \quad (3.12)$$

For this choice of λ we get when $\tau_Q \leq T$ the payoff (here use that $\lambda_{yy} = 2/y^2$)

$$\frac{1}{2} \int_{\tau_Q}^T \lambda_{yy}(S_t) d\langle S \rangle_t = \int_{\tau_Q}^T \frac{d\langle S \rangle_t}{S_t^2} = \langle X \rangle_T - Q,$$

and when $\tau_Q > T$ the payoff

$$-BS(S_T, Q - \langle X \rangle_T; \lambda) + BS(S_T, 0; \lambda) = \langle X \rangle_T - Q.$$

where we have used the fact that

$$BS(S_T, 0; \lambda) = \lambda(S_T) = -2 \log(S_T/S_0) + 2 \frac{S_T - S_0}{S_0} \quad (3.13)$$

and (letting $p(z)$ be the probability density function of $\mathcal{N}(-v/2, v)$, where $v = (Q - \langle X \rangle_T)$)

$$\begin{aligned} BS(S_T, Q - \langle X \rangle_T; \lambda) &= \int_{-\infty}^\infty \left[-2 \log(S_T e^z / S_0) + 2 \frac{S_T e^z - S_0}{S_0} \right] p(z) dz \\ &= BS(S_T, 0; \lambda) - 2 \int_{-\infty}^\infty z p(z) dz = BS(S_T, 0; \lambda) + Q - \langle X \rangle_T. \end{aligned} \quad (3.14)$$

We thus see that for this specific choice of λ , the subhedging strategy actually allows us to perfectly replicate a variance swap.

Now, consider the ‘‘optimal choice’’ of λ (attributed to Dupire [26]), specified in Proposition 3.1. The intuition behind why this choice is optimal can be seen by the following argument. By using e.g. (2.11), we may rewrite the lower bound (see Carr & Lee [7]) as

$$\begin{aligned} \mathbb{E}\lambda(S_T) - BS(S_0, Q; \lambda) \\ = \int_0^\infty \lambda_{yy}(K) [BS(S_0, I_0(K, T); \text{van}_K) - BS(S_0, Q; \text{van}_K)] dK. \end{aligned} \quad (3.15)$$

Let $\mathcal{A} := \{K : I_0(K, T) > Q\}$, and differentiate the optimal λ twice to get

$$\begin{aligned}\lambda(y) &= \int_{\mathcal{A} \cap (S_0, \infty)} \frac{2}{K^2} (y - K)^+ dK + \int_{\mathcal{A} \cap (0, S_0]} \frac{2}{K^2} (K - y)^+ dK \\ \lambda_y(y) &= \int_{\mathcal{A} \cap (S_0, \infty)} \frac{2}{K^2} \mathbb{1}_{\{y \geq K\}} dK - \int_{\mathcal{A} \cap (0, S_0]} \frac{2}{K^2} \mathbb{1}_{\{K > y\}} dK \\ \lambda_{yy}(y) &= \int_{\mathcal{A} \cap (S_0, \infty)} \frac{2}{K^2} \delta(y - K) dK + \int_{\mathcal{A} \cap (0, S_0]} \frac{2}{K^2} \delta(y - K) dK \\ &= \int_{\mathcal{A}} \frac{2}{K^2} \delta(y - K) dK = \frac{2}{y^2} \mathbb{1}_{\{y : I_0(y, T) > Q\}}(y).\end{aligned}$$

We may thus think of the optimal λ as starting from the λ that replicates a variance swap, and then modifying the domain of strikes that we integrate over in such a way that we only allow positive contributions to the lower bound (3.15) (recall that $BS(y, v; \lambda)$ is increasing in its second argument, so $I_0(K, T) > Q$ is equivalent to a non-negative integrand).

(b) Superhedging strategy

In analogy with the case for the lower bound, Carr & Lee [7] devise a superhedging strategy in order to find an upper bound on the value of the variance option. Their main results for the upper bound are presented in Proposition 3.2.

Proposition 3.2. (*Carr & Lee [7]*). *Define the function L^* by*

$$L^*(y, b_d, b_u, Q) := \begin{cases} L(y; b_d, b_u) & \text{if } y \notin (b_d, b_u), \\ -BP(y, 0; b_d, b_u, Q) & \text{if } y \in (b_d, b_u), \end{cases} \quad (3.16)$$

where

$$L(y; b_d, b_u) := \begin{cases} -2 \log(y/b_u) + 2 \frac{\log(b_u/b_d)}{b_u - b_d} (y - b_u) & \text{if } b_d \neq b_u, \\ -2 \log(y/S_0) + 2y/S_0 - 2 & \text{if } b_d = b_u = S_0, \end{cases} \quad (3.17)$$

and (letting $\zeta = \sqrt{1/4 - 2iz}$)

$$BP(y, q; b_d, b_u, Q) = \int_{-\infty - \alpha i}^{\infty - \alpha i} \frac{\sqrt{y/b_u} \sinh(\log(b_d/y)\zeta) - \sqrt{y/b_d} \sinh(\log(b_u/y)\zeta)}{2\pi z^2 e^{i(Q-q)z} \sinh(\log(b_u/b_d)\zeta)} dz. \quad (3.18)$$

Then for each choice of b_d and b_u with $0 < b_d \leq S_0 \leq b_u < \infty$, the expression

$$-L^*(S_0; b_d, b_u, Q) + \mathbb{E} L^*(S_T; b_d, b_u, Q) \quad (3.19)$$

is an upper bound on the no-arbitrage price of the variance call with payoff $(\langle X \rangle_T - Q)^+$.

The Carr & Lee upper bound in Proposition 3.2 is in fact the time-0 value of a strategy superhedging the variance call payoff $(\langle X \rangle_T - Q)^+$, and so can be taken as an upper bound on the no-arbitrage price of the variance call.

As stated in Carr & Lee [7], the interpretation of the function BP above is as the expected value of $(\langle X \rangle_{\tau_\beta} - Q)^+$ with τ_β being the first time that the price process S exits the chosen interval (b_d, b_u) . Unlike the case for the subhedging strategy where the optimal λ is chosen, there remains some room for optimisation over b_d and b_u , and it is possible (and likely) that our choice of values for these in our numerical implementation in Chapter 4 will be suboptimal.

3.2 The Cox & Wang approach

Dupire [27] showed that the Root and Rost barriers can be characterised in terms of solutions to certain free boundary problems. Cox & Wang further developed the characterisation of the Root barrier in [13], where they also derived a corresponding subhedging strategy. In [12], they show how the Rost barrier can be constructed, together with a superhedging strategy. Gassiat et al. [28] extend the theory for PDE characterisation of Root and Rost barriers by using viscosity solutions, and we will use some of the results from Gassiat et al. for our numerical implementation in Chapter 4.

(a) Root embedding and subhedging

In the context of Gassiat et al. [28], let $(\Omega, \mathcal{F}, \{\mathcal{F}_t\}, \mathbb{P})$ be a filtered probability space and W a standard Brownian motion on this space. Let $Z_0 \sim \nu$ be a random variable on \mathbb{R} independent of W , and let the process Z have the dynamics

$$dZ_t = \sigma(t, Z_t)dW_t, \quad Z_0 \sim \nu. \quad (3.20)$$

We summarise the relevant results from [28] in Theorem 3.3.

Theorem 3.3. (*Gassiat et al. [28]*) *Assume that ν and μ are probability measures on $(\mathbb{R}, \mathcal{B}(\mathbb{R}))$ such that they have a first moment and that their potentials satisfy*

$$U_\mu(x) \leq U_\nu(x), \quad \forall x \in \mathbb{R}. \quad (3.21)$$

Furthermore, let $\sigma(t, x) \in \mathcal{C}([0, \infty), \mathbb{R})$ satisfy the Lipschitz and linear growth conditions

$$\sup_{t \in [0, \infty)} \sup_{x \neq y} \frac{|\sigma(t, x) - \sigma(t, y)|}{|x - y|} < \infty, \quad \sup_{t \in [0, \infty)} \sup_{x \in \mathbb{R}} \frac{|\sigma(t, x)|}{1 + |x|} < \infty, \quad (3.22)$$

and further assume that for each compact $K \subset \{x : U_\nu(x) \neq U_\mu(x)\}$ we can find a constant $c_K > 0$ such that $\sigma(t, x) \geq c_K > 0$, $\forall t \geq 0$, $x \in K$ (local ellipticity).

Under the above assumptions, the following two conditions are equivalent:

1. *there exists a Root barrier R such that the hitting time $\tau_R = \inf\{t > 0 : (t, Z_t) \in R\}$ embeds μ in Z ,*
2. *there exists a time decreasing viscosity solution $u \in \mathcal{C}([0, \infty], [-\infty, \infty])$ to the problem*

$$\begin{cases} \min(u - U_\mu, \partial_t u - \frac{\sigma(x)^2}{2} \partial_{xx} u) = 0 & \text{on } (0, \infty) \times \mathbb{R}, \\ u(0, x) = U_\nu(x), \\ u(\infty, x) = U_\mu(x). \end{cases} \quad (3.23)$$

In addition, the Root barrier is found as

$$R = \{(t, x) \in [0, \infty] \times [-\infty, \infty] : u(t, x) = U_\mu(x)\} \quad (3.24)$$

and we have

$$u(t, x) = -\mathbb{E}|Z_{\tau_R \wedge t} - x|. \quad (3.25)$$

Recall that the assumption $U_\mu(x) \leq U_\nu(x)$, $\forall x \in \mathbb{R}$ is required for Theorem 2.6 to ensure the existence of a stopping time of minimal residual expectation, and that by Theorem 2.7 every Root stopping time is of minimal residual expectation.

Furthermore, since we are trying to embed the implied distribution μ in the geometric Brownian motion $dZ_t = Z_t dW_t$, $Z_0 \sim \nu$, we will be especially interested in the case $\sigma(t, x) = x$. This choice of σ is sufficiently smooth and satisfies both the Lipschitz and linear growth conditions (3.22). The local ellipticity is more subtle in this case, and as stated in Gassiat et al. [28], it holds for $\sigma(t, x) = x$ if and only if $\text{supp}(\mu) \subset \mathbb{R}_+$.

Thus, given that the distributions ν and μ satisfy (3.21), we may find the Root barrier embedding μ in Z from the solution to the free boundary problem (3.23). Given a solution to (3.23), we can construct the stopping time $\tau_R = \inf\{t > 0 : (t, Z_t) \in R\}$ using the characterisation (3.24), and then use the law of this stopping time to determine $\mathbb{E}[(\tau_R - Q)^+]$. Therefore, solving the free boundary problem (3.23) will allow us to find a lower price bound on the variance call.

We now turn to the subhedging strategy from Cox & Wang [13]. Consider the case of embedding μ in Z defined in (3.20), where σ is smooth, satisfies the Lipschitz condition, and $\exists K > 0$ such that $1/K < \sigma < K$ on \mathbb{R} . Let F be a convex increasing payoff function with $F(0) = 0$ and denote by f its right derivative. Furthermore, introduce

$$M(x, t) = \mathbb{E}^{(x, t)} f(\tau_R) \quad (3.26)$$

and assume that M is locally bounded on $\mathbb{R} \times \mathbb{R}_+$. Here $\mathbb{E}^{(x, t)}$ is the expectation if we start the process that we embed in at x at time t , and τ_R is the Root stopping time. Furthermore, define the functions

$$Z(x) = 2 \int_0^x \int_0^y \frac{M(z, 0)}{\sigma(z)^2} dz dy, \quad (3.27)$$

$$G(x, t) = \int_0^t M(x, s) ds - Z(x), \quad (3.28)$$

$$H(x) = \int_0^{R(x)} (f(s) - M(x, s)) ds + Z(x), \quad (3.29)$$

and notice that since $Z''(x) = 2 \frac{M(x, 0)}{\sigma(x)^2} > 0$, we have that Z is convex. Then by Cox & Wang [13], we have $G(x, t) + H(x) \leq F(t)$, $\forall (x, t) \in \mathbb{R} \times \mathbb{R}_+$, which will allow us to use G and H to subhedge F . Finally, define $\tau_t := \int_0^t \sigma_s^2 ds$, and $\phi_t := \tilde{\phi}_{\tau_t}$ where $\tilde{\phi}_t \in [\frac{\partial G}{\partial x}(x-, t), \frac{\partial G}{\partial x}(x+, t)]$. Then the strategy of holding at each time t

$$\left\{ \begin{array}{l} \phi_t + H'_+(S_0) \text{ shares of the asset,} \\ G(S_0, 0) - \phi_0 S_0 + H(S_0) - H'_+(S_0) S_0 \text{ bonds,} \\ H''(dK) \text{ units of the call with strike } K \text{ for } K \in (S_0, \infty), \\ H''(dK) \text{ units of the put with strike } K \text{ for } K \in (0, S_0]. \end{array} \right. \quad (3.30)$$

subhedges the payoff $F(\langle X \rangle_T)$, and this is the subhedging strategy of Cox & Wang [13]. The subhedging cost, i.e. the cost of setting up this portfolio, is given by

$$G(S_0, 0) + H(S_0) + \int_0^{S_0} P_0(K) H''(dK) + \int_{S_0}^\infty C_0(K) H''(dK), \quad (3.31)$$

and this would then be a lower bound on the no-arbitrage price of the variance call.

Remark 3.4. Our case of interest $\sigma(x) = x$ does not satisfy the condition $1/K < \sigma < K$ for some $K > 0$ and all $x \in \mathbb{R}$. Nevertheless, the results of Cox & Wang can be extended to this case as long as we only allow values on $(0, \infty)$ [13].

Remark 3.5. The subhedging property of the above strategy in fact holds for any choice of barrier function $R(x)$ (without requiring that they embed the target distribution), and we choose the Root barrier in order to determine the optimal (highest possible) value of the lower bound [13].

(b) Rost embedding and superhedging

The Rost embedding can be described using a PDE formulation similar to that for Root above. The relevant results from Gassiat et al. [28] are presented in Theorem 3.6 below.

Theorem 3.6. (Gassiat et al. [28]) *Assume that ν , μ , and $\sigma(t, x)$ satisfy the assumptions of Theorem 3.3. Then the statement 1. below implies statement 2.:*

1. *there exists a Rost barrier \bar{R} such that the hitting time $\tau_{\bar{R}} = \inf\{t > 0 : (t, Z_t) \in \bar{R}\}$ embeds μ in Z ,*
2. *there exists a time decreasing viscosity solution $u \in \mathcal{C}([0, \infty], [-\infty, \infty])$ to the problem*

$$\begin{cases} \partial_t u = \min\left(0, \frac{\sigma(x)^2}{2} \partial_{xx} u\right) & \text{on } (0, \infty) \times \mathbb{R}, \\ u(0, x) = U_\nu(x) - U_\mu(x). \end{cases} \quad (3.32)$$

If we further assume that there exists an open set V such that

$$\text{supp}(\nu) \subset V \subset \text{supp}(\mu)^c \quad (3.33)$$

holds, then we also have that 2. implies 1.

The Rost barrier can then be found as

$$\bar{R} = \{(t, x) \in (0, \infty) \times \mathbb{R} : u(t, x) = u(0, x)\} \quad (3.34)$$

and we have

$$u(t, x) = -\mathbb{E}|Z_{\tau_{\bar{R}} \wedge t} - x| - U_\mu(x). \quad (3.35)$$

Remark 3.7. The condition (3.33) can be intuitively thought of in the following way: consider embedding $\mathcal{N}(0, 1)$ in a process Y with $Y_0 \sim \mathcal{U}([-0.5, 0.5])$. For the supports of these distributions we have

$$\text{supp}\left(\mathcal{U}([-0.5, 0.5])\right) = [-0.5, 0.5] \subset \mathbb{R} = \text{supp}(\mathcal{N}(0, 1)), \quad (3.36)$$

and they thus overlap. Due to the definition of a reversed barrier, the only way to embed the values from the interval $[-0.5, 0.5]$ would be to have the barrier overlap that interval, and we would thus stop the process at time zero, preventing embedding of the desired target distribution.

In a similar fashion as for the Root barrier, the solution to the free boundary problem (3.32) in Theorem 3.6 allows us to characterise the Rost barrier. Given that the conditions in the theorem hold, once we have found a solution to (3.32) we can then write the barrier as $\bar{R} = \{(t, x) \in (0, \infty] \times \mathbb{R} : u(t, x) = u(0, x)\}$, and construct the Rost stopping time $\tau_{\bar{R}} = \inf\{t > 0 : (t, Z_t) \in \bar{R}\}$. Knowing the law of this stopping time, we can then determine the upper bound $\mathbb{E}[(\tau_{\bar{R}} - Q)^+]$ on the price of the variance call.

The Cox & Wang superhedging strategy follows the same general structure as their subhedging strategy. Let M be defined as in (3.26), with the Rost stopping time $\tau_{\bar{R}}$ in place of the Root τ_R , and as before assume local boundedness. Assume that $\Gamma := \lim_{t \rightarrow \infty} f(t) < \infty$ exists, and define (for some $S_0^* \in (\inf \text{supp}(\mu), \inf \text{supp}(\mu))$) the functions

$$Q(x) = \int_{S_0^*}^x \int_{S_0^*}^y \frac{2}{\sigma(z)^2} dz dy, \quad (3.37)$$

$$J(x, t) = \lim_{T \rightarrow \infty} \int_t^T [M(x, s) - f(s)] ds, \quad (3.38)$$

$$G(x, t) = F(t) - J(x, t) - \Gamma Q(x), \quad (3.39)$$

$$H(x) = J(x, R(x)) + \Gamma Q(x). \quad (3.40)$$

Again, let $\phi_t := \tilde{\phi}_{\tau_t}$ and $\tilde{\phi}_t \in [\frac{\partial G}{\partial x}(x-, t), \frac{\partial G}{\partial x}(x+, t)]$. Then, the strategy (3.30) with the alternative definitions of G and H as in (3.39) and (3.40) superhedges the payoff $F(\langle X \rangle_T)$ [12].

3.3 Comparing the approaches theoretically

(a) General observations

In the previous two sections we have presented two alternative approaches for bounding the no-arbitrage of variance calls, and we will here compare them from a theoretical point of view. We will particularly investigate the connection between the methods for obtaining lower bounds.

As an initial observation, the approach of Cox & Wang [12, 13] will generally give tighter bounds on the no-arbitrage price than that of Carr & Lee [7]. The optimality of the Root and Rost embeddings implies that their corresponding price bounds are as tight as possible, in the sense that they can each be associated with some admissible arbitrage free model for the price process, and that $\mathbb{E}(\tau_R - Q)^+ \leq \mathbb{E}(\tau - Q)^+ \leq \mathbb{E}(\tau_{\bar{R}} - Q)^+$ for all solutions τ to the SEP. Hence, making the bounds tighter than the Root and Rost bounds would introduce arbitrage in their associated models. The bounds from the Carr & Lee approach, however, do not have the same optimality property as the Root and Rost embeddings, and so we may think of it in the general case as an approximate method. The general idea behind the Carr & Lee approach is to find a lower bound on the supremum over the subhedging strategies, and an upper bound on the infimum over the superhedging strategies, without necessarily attaining either extremum. Put differently, Carr & Lee work within a subset of the family of subhedging strategies and try to maximise their strategy in order to approach

the optimal lower bound from below, while Cox & Wang do attain the supremum (and vice versa for the upper bound).

The results for bounding the values of variance calls presented above can be extended to larger classes of payoffs. As explained in Section 2.3, put-call parity for variance options allows us to directly extend the results to variance puts. Using the fact the Root and Rost stopping times maximise and minimise the quantity $\mathbb{E}F(\tau)$ for convex F , the idea of the Cox & Wang approach can be generalised to convex payoffs, with a trivial extension to the concave case.

Furthermore, both approaches can be used to obtain price bounds for a larger class of derivatives by using the following arguments. Consider a twice differentiable payoff $F(x)$. Then using (2.11), F may be decomposed as

$$\begin{aligned} F(\langle X \rangle_T) &= F(S_0) + F'(S_0)[\langle X \rangle_T - S_0] + \int_{S_0}^{\infty} F''(K)(\langle X \rangle_T - K)^+ dK \\ &\quad + \int_0^{S_0} F''(K)(K - \langle X \rangle_T)^+ dK. \end{aligned} \tag{3.41}$$

The variance put can be rewritten using put-call parity (2.15), so that the decomposition becomes

$$\begin{aligned} F(\langle X \rangle_T) &= F(S_0) + F'(S_0)[\langle X \rangle_T - S_0] + \int_{S_0}^{\infty} F''(K)(\langle X \rangle_T - K)^+ dK \\ &\quad + \int_0^{S_0} F''(K)[(\langle X \rangle_T - K)^+ + K - \langle X \rangle_T] dK \\ &= \left[F(S_0) - S_0 F'(S_0) + \int_0^{\infty} K F''(K) dK \right] + \left[F'(S_0) - \int_0^{\infty} F''(K) dK \right] \langle X \rangle_T \\ &\quad + \int_0^{\infty} F''(K)(\langle X \rangle_T - K)^+ dK. \end{aligned}$$

Define

$$w_B = F(S_0) - S_0 F'(S_0) + \int_0^{\infty} K F''(K) dK \tag{3.42}$$

$$w_X = F'(S_0) - \int_0^{\infty} F''(K) dK, \tag{3.43}$$

so that we may write the payoff as

$$F(\langle X \rangle_T) = w_B + w_X \langle X \rangle_T + \int_0^{\infty} F''(K)(\langle X \rangle_T - K)^+ dK. \tag{3.44}$$

The first term in the RHS is a constant and can be replicated by bonds, and the second term can be replicated using (2.10) and (2.12). In the final term, we have a combination of variance calls, which we may sub- or superhedge using e.g. Carr & Lee or Cox & Wang. In order to obtain a lower bound, we can subhedge the calls at all strikes K where $F''(K) \geq 0$ and superhedge calls at all strikes K where $F''(K) < 0$, and vice versa to obtain an upper bound.

Note that both Carr & Lee [7] and Cox & Wang [12,13] work in the setting of continuous price processes. For a treatment of the case when jumps are allowed in the underlying process, see e.g. Hobson & Klimmek [33].

(b) Carr & Lee subhedge as a special case of Root embedding

We will now turn to one of our main interests for this section, which is investigating in what sense the Carr & Lee subhedging strategy can be thought of as an approximation of the Cox & Wang subhedging, and in what settings we expect them to be equivalent. As stated in Remark 5.4 in Cox & Wang [13], the lower bound from the Carr & Lee subhedging [7] may be considered a special case of the Cox & Wang subhedging where we choose a constant barrier function $R(x) = Q$ instead of the Root barrier. It is this connection that we here explore and characterise.

First, consider the case of a log-normal target distribution μ , for which we assume $\int x\mu(dx) = S_0$, which is a necessary condition for $U_\nu \geq U_\mu$ and thus Theorem 2.6. Such a target distribution arises from e.g. the Black-Scholes dynamics. Proposition 3.8 says that for such distributions, the Carr & Lee subhedging is an exact hedging strategy. It is worth noting that not only does the lower bound from the Carr & Lee subhedging in this case coincide with the Root bound, but they both yield the “true” price of the variance call.

Proposition 3.8. *If the target distribution μ of the price process is log-normal (with $\int x\mu(dx) = S_0$), then the Carr & Lee subhedging strategy perfectly replicates the variance call payoff.*

Proof. Since we are embedding the distribution in the geometric Brownian motion $Z_t = S_0 \exp(W_t - t/2)$, which has mean S_0 , the variance (parameterised by t) is the only degree of freedom left for the log-normal μ . In other words, for each time t , the distribution of Z_t is log-normal with mean S_0 and variance $S_0^2(e^t - 1)$. Hence, the Root barrier for embedding μ in Z will be some constant $q > 0$, with associated martingale process $\tilde{S}_t := Z_{q \wedge \frac{t}{T-t}}$, and we have $\tilde{S}_0 = S_0$ and $\tilde{S}_T = Z_q \sim \mu$. Equivalently, any constant barrier $R(x) = q$ will embed a log-normal distribution in Z . Note that with the Black-Scholes model, we would set $q = \sigma^2 T$.

We now examine how the Carr & Lee subhedging strategy performs for this martingale process. We have $\langle X \rangle_T = \langle \log Z \rangle_q = q$. Thus if $q \geq Q$, we have $\tau_Q \leq T$, and else $\tau_Q > T$. In the case of $q \geq Q$, we have from the fact that the target distribution is log-normal that $I_0(K, T) = q \geq Q$ for all K , and we thus get the payoff

$$\frac{1}{2} \int_{\tau_Q}^T \lambda_{yy}(S_t) d\langle S \rangle_t \leq \frac{1}{2} \int_{\tau_Q}^T d\langle \log S \rangle_t = q - Q = (q - Q)^+, \quad (3.45)$$

with equality if we choose λ as in (3.7). If on the other hand $q < Q$, we instead get the payoff

$$-BS(Z_q, Q - q; \lambda) + BS(Z_q, 0; \lambda). \quad (3.46)$$

However, since in this case $I_0(K, T) = q < Q$ for all K , the integral in the optimal λ (3.7) will be over a null set, whereby we get

$$-BS(Z_q, Q - q; \lambda) + BS(Z_q, 0; \lambda) = 0 = (q - Q)^+. \quad (3.47)$$

Hence, the Carr & Lee subhedge will always perfectly replicate variance call payoffs whenever we embed in Z and the Rost barrier function $R(x)$ is a constant, i.e. when the target distribution is log-normal. \square

Furthermore, we have by Theorem 3.9 that the Cox & Wang subhedging strategy indeed reduces to the Carr & Lee subhedging strategy if we use a constant barrier function $R(x) = Q$ instead of the Root barrier function, without making any additional assumptions about the target distribution.

Theorem 3.9. *(Based on Remark 5.4 in Cox & Wang [13]) When using $R(x) = Q$ instead of the Root barrier, the Cox & Wang subhedging reduces to a Carr & Lee subhedging strategy with λ as in (3.11). If $I_0(K, T) > Q$ for all K , then the modified Cox & Wang strategy reduces to the optimal Carr & Lee subhedging (with λ as in (3.7)).*

The proof of Theorem 3.9 will be given at the end of this chapter, and we will first prove Lemma 3.10 below. As mentioned in Remark 3.4, the results of Cox & Wang can be extended to the case of $\sigma(x) = x$. In this case, a lower limit of integration of zero in (3.27) causes the integral to diverge. Note that Cox & Wang [13] never use the fact that the lower limit of integration is zero in their proofs, and so we are able to change the lower limit as in Lemma 3.10.

Lemma 3.10. *In the case of $\sigma(x) = x$, a constant barrier function $R(x) = Q$, and F a call payoff, the Cox & Wang subhedging strategy is unchanged if we instead use $Z(x) = 2 \int_{S_0}^x \int_{S_0}^y z^{-2} dz dy$.*

Proof. Consider the Cox & Wang subhedging strategy (3.30) with Z , G , and H defined as in (3.27), (3.28), and (3.29). The time- t value of this subhedging portfolio is then

$$\begin{aligned}
& G(S_0, 0) + \int_0^t \phi_s dS_s + H(S_0) + H'_+(S_0)(S_t - S_0) + \int_0^{S_0} P_t(K) H''(dK) \\
& \quad + \int_{S_0}^{\infty} C_t(K) H''(dK) \\
& = G(S_0, 0) + \int_0^t \phi_s dS_s + \mathbb{E}_t \left[H(S_0) + H'_+(S_0)(S_T - S_0) + \int_0^{S_0} (K - S_T)^+ H''(dK) \right. \\
& \quad \left. + \int_{S_0}^{\infty} (S_T - K)^+ H''(dK) \right] \\
& = G(S_0, 0) + \int_0^t \phi_s dS_s + \mathbb{E}_t [H(S_T)], \tag{3.48}
\end{aligned}$$

where we used (2.11) in the last equality. For the call payoff $F(x) = (x - Q)^+$ we have the right derivative

$$f(x) = \begin{cases} 1 & \text{if } x \geq Q, \\ 0 & \text{if } x < Q, \end{cases} \tag{3.49}$$

and with $R(x) = Q$ we now get

$$M(x, t) = \mathbb{E}^{(x,t)} f(Q) = 1. \tag{3.50}$$

Rewrite Z as

$$\begin{aligned} Z(x) &= 2 \int_0^x \left[\int_\kappa^y \frac{1}{z^2} dz + \int_0^\kappa \frac{1}{z^2} dz \right] dy \\ &= 2 \int_\kappa^x \int_\kappa^y \frac{1}{z^2} dz dy + 2 \int_0^\kappa \left[\frac{1}{S_0} - \frac{1}{y} \right] dy + 2x \int_0^\kappa \frac{1}{z^2} dz. \end{aligned} \quad (3.51)$$

If we now define

$$g_\kappa(x) := 2 \int_0^\kappa \left[\frac{1}{S_0} - \frac{1}{y} \right] dy + 2x \int_0^\kappa \frac{1}{z^2} dz, \quad (3.52)$$

$$Z_\kappa(x) := 2 \int_\kappa^x \int_\kappa^y \frac{1}{z^2} dz, \quad (3.53)$$

so that

$$Z(x) = Z_\kappa(x) + g_\kappa(x), \quad (3.54)$$

then the time- t value of the portfolio becomes (note that g_κ is a linear function in x)

$$G(S_0, 0) + \int_0^t \phi_s dS_s + \mathbb{E}_t[H(S_T)] \quad (3.55)$$

$$= -Z_\kappa(S_0) - g_\kappa(S_0) - \int_0^t \left[Z'_\kappa(S_s) + g'_\kappa(S_s) \right] dS_s + \mathbb{E}_t[-Q + Z_\kappa(S_T) + g_\kappa(S_T)] \quad (3.56)$$

$$= \mathbb{E}_t[Z_\kappa(S_T)] - Q - Z_\kappa(S_0) - \int_0^t Z'_\kappa(S_s) dS_s + g(S_t) - g(S_0) - \int_0^t g'(S_s) dS_s \quad (3.57)$$

$$= \mathbb{E}_t[Z_\kappa(S_T)] - Q - Z_\kappa(S_0) - \int_0^t Z'_\kappa(S_s) dS_s. \quad (3.58)$$

So far, $\kappa > 0$ has been an arbitrary constant. We will now show that we can take $\kappa = S_0$ without any loss of generality. To do this, we repeat the steps in (3.51) (or simply use $Z(x) = Z_\kappa(x) + g_\kappa(x) = Z_{S_0}(x) + g_{S_0}(x)$) to get

$$Z_\kappa(x) = Z_{S_0}(x) + g_{S_0}(x) - g_\kappa(x), \quad (3.59)$$

and from this we arrive at

$$\mathbb{E}_t[Z_\kappa(S_T)] - Q - Z_\kappa(S_0) + \int_0^t Z'_\kappa(S_s) dS_s = \mathbb{E}_t[Z_{S_0}(S_T)] - Q - Z_{S_0}(S_0) + \int_0^t Z'_{S_0}(S_s) dS_s. \quad (3.60)$$

□

Having shown Lemma 3.10, we now turn to the proof of Theorem 3.9.

Proof of Theorem 3.9. Recall Remark 3.5 that the Cox & Wang strategy subhedges for any choice of $R(x)$, and that choosing the Root barrier maximises the lower bound. We thus take $R(x) = Q$ and still obtain a subhedging portfolio. By Lemma 3.10, we may then use a modified Z of the form

$$Z(x) = 2 \int_{S_0}^x \int_{S_0}^y \frac{1}{z^2} dz dy \quad (3.61)$$

for the subhedging, and we get

$$Z(x) = 2 \int_{S_0}^x \left[\frac{1}{S_0} - \frac{1}{y} \right] dy = 2 \left[\frac{x - S_0}{S_0} - \log(x/S_0) \right]. \quad (3.62)$$

If we choose λ as in (3.11), we can further simplify Z to $Z(x) = \lambda(x)$. Moreover, we have

$$G(x, t) = \int_0^t ds - Z(x) = t - Z(x), \quad (3.63)$$

$$H(x) = \int_0^Q (\mathbb{1}_{\{s \geq Q\}} - 1) ds + Z(x) = -Q + Z(x), \quad (3.64)$$

and the time- t value (3.48) of the Cox & Wang subhedging portfolio can thus be written

$$Z(S_0) + \int_0^t \phi_s dS_s + \mathbb{E}_t[-Q + Z(S_T)] = \mathbb{E}_t[\lambda(S_T)] - Q + \int_0^t \phi_s dS_s. \quad (3.65)$$

Now, with λ as in (3.11), we may use (3.14) to obtain

$$BS(S_0, Q; \lambda) = Q. \quad (3.66)$$

In addition, if we take $\phi_t = \frac{\partial G}{\partial x}(S_t, \tau_t)$ we get (using (3.62))

$$\phi_t = -Z'(S_T) = \frac{2}{S_t} - \frac{2}{S_0}. \quad (3.67)$$

Comparing this with N_t defined in (3.3), we find that (using the same $p(z)$ as in (3.14))

$$\lambda_y(y) = -\frac{2}{y} + \frac{2}{S_0}, \quad (3.68)$$

$$BS_y(y, v; \lambda) = \int_{-\infty}^{\infty} \left[-\frac{2}{y} + \frac{2}{S_0} e^z \right] p(z) dz = -\frac{2}{y} + \frac{2}{S_0}, \quad (3.69)$$

and thus $\phi_t = N_t$. Then the time- t of the portfolio is

$$\mathbb{E}[\lambda(S_T)] + N_t S_t - BS(S_0, Q; \lambda) + \int_0^t N_s dS_s - N_t S_t, \quad (3.70)$$

which is equivalent to the Carr & Lee subhedging strategy (3.4). Hence, we have shown that when using $R(x) = Q$, the Cox & Wang subhedging reduces to a Carr & Lee subhedging strategy with λ as in (3.11). If $I_0(K, T) > Q$ for all K , then we may also use the optimal λ from (3.7) in our arguments above, whereby the modified Cox & Wang strategy would reduce to the optimal Carr & Lee subhedging. This concludes the proof. \square

Chapter 4. Numerical investigation

We here investigate how the approaches by Carr & Lee [7] and Cox & Wang [12,13] perform in numerically simulated scenarios. The structure of this chapter is as follows: in Section 4.1 we explain the strategy we employ to generate our simulated data; in Sections 4.2 and 4.3 we describe our implementation and results for the Carr & Lee and Cox & Wang approaches respectively; and in Section 4.4 we compare and discuss the results. The MATLAB code for our implementation is available upon request.

4.1 Simulating data

To compare the two approaches numerically, we test them on simulated data for which we may also determine the “true” variance call value.

Recall the Black-Scholes dynamics as given in (2.1), and the Heston model dynamics as in (2.2). Based on the discussion in Section 2.3, we set the interest rate r to be zero in both models. The price processes are then martingales, and there is no need to discount future values using bond prices.

There are three kinds of data that we need to synthesise in order to carry out our analysis: (i) price paths; (ii) terminal distributions; and (iii) European call option prices. In simple cases, these three can be determined by independent computations, but in more general setups we may need to compute some of them based on the others. In our implementation, we start by computing call prices over a range of strikes under the chosen model (Black-Scholes or Heston), and then find the implied distribution from the call prices. We take this implied distribution as the target distribution when determining the price bounds, and path simulation is used to find the “true prices” for the variance calls. A more detailed description of these steps is provided below.

(a) Path simulation

For the Black-Scholes model, we have paths of the form

$$S_t = S_0 \exp\left(-\frac{1}{2}\sigma^2 t + \sigma W_t\right) \quad (4.1)$$

for a standard Brownian motion W . If we simulate these paths with a time-step of Δt , then we can generate independent Brownian increments $\Delta W_n \sim \mathcal{N}(0, \Delta t)$ and simply compute each simulated value \widehat{S}_n along the path as

$$\widehat{S}_n = S_0 \exp\left(-\frac{1}{2}\sigma^2 n\Delta t + \sigma \sum_{i=1}^n \Delta W_i\right). \quad (4.2)$$

Heston paths are simulated using the following scheme [37, 41]:

$$v_{n+1} = v_n + \kappa(\theta - v_n^+) \Delta t + \varsigma \sqrt{v_n^+} \Delta \widehat{W}_n, \quad (4.3)$$

$$S_{n+1} = S_n \exp\left(-v_n^+ / 2 \Delta t + \sqrt{v_n^+} \Delta W_n\right), \quad (4.4)$$

where \widehat{W} and W have correlation ρ .

As for parameter values, we take maturity $T = 2$ and initial price of the underlying $S_0 = 100$ for both models. For the Black-Scholes model, we will take $\sigma = 0.2$. We use the same Heston parameter values as in Carr & Lee [7], which are $\kappa = 1.15$, $\theta = 0.04$, $\varsigma = 0.39$, $v_0 = 0.04$, and $\rho = 0$. Note that the Feller condition is not satisfied for these values, so that we do need the truncation v_n^+ in (4.3), and that W and \widehat{W} become uncorrelated.

In the Black-Scholes case, the realised variance is trivially $\int_0^T \sigma^2 dt = \sigma^2 T$. For the Heston paths, we instead compute the realised variance of each simulated path using the discretisation in (2.7), where we take the t_i to be the discrete times in our simulation.

(b) Determining distributions

For the Black-Scholes models, the price process will have a log-normal distribution at maturity T , and for the Heston model we can find a semi-closed expression [22] for the probability density function. An alternative approach to using the closed and semi-closed expressions is to apply the Breeden-Litzenberger formula to the call prices to determine the implied density, and this is a method of obtaining the terminal (implied) distribution without having to know the underlying dynamics. For this reason, this latter method appeals to the idea of model-independent pricing.

Discretise the strikes over a grid $[K_{min}, K_{max}]$ with a step size of ΔK . We then apply the Breeden-Litzenberger formula (2.16) and approximate the implied density $\widehat{p}(K)$ at discrete points using the finite difference scheme

$$\widehat{p}(K) = \frac{C(K + \Delta K) - 2C(K) + C(K - \Delta K)}{\Delta K^2}. \quad (4.5)$$

This would then correspond to the target distribution that we aim to embed in our numerical implementation.

(c) Computing European call option prices

For the Black-Scholes model we directly obtain the European call option prices using the formula

$$C(S, t; K, T) = S_0 \Phi(d_1) - K \Phi(d_2), \quad (4.6)$$

where

$$d_1 = \frac{\log(S_0/K) + \frac{1}{2}\sigma^2 T}{\sigma\sqrt{T}}, \quad d_2 = d_1 - \sigma\sqrt{T}, \quad (4.7)$$

and Φ is the standard normal cumulative density function. For the Heston model, we will use the method below (based on [31], where we have set $r = \rho = 0$):

$$C(S, v, t; K, T) = S_0 P_1 - K P_2 \quad (4.8)$$

$$P_j(x, v, T; \log(K)) = \frac{1}{2} + \frac{1}{\pi} \int_0^\infty \operatorname{Re} \left[\frac{e^{-i\phi \log(K)} f_j(x, v, T; \phi)}{i\phi} \right] d\phi \quad (4.9)$$

with

$$f_j(x, v, t; \phi) = \exp(C_j(T - t; \phi) + D_j(T - t; \phi)v + i\phi x), \quad (4.10)$$

$$C_j(\tau; \phi) = \frac{a}{\zeta^2} \left\{ (b + d_j)\tau - 2 \log \left[\frac{1 - g_j e^{d_j \tau}}{1 - g_j} \right] \right\} \quad (4.11)$$

$$D_j(\tau; \phi) = \frac{b + d_j}{\zeta^2} \left[\frac{1 - e^{d_j \tau}}{1 - g_j e^{d_j \tau}} \right], \quad (4.12)$$

and

$$g_j = \frac{b + d_j}{b - d_j}, \quad (4.13)$$

$$d_j = \sqrt{b^2 - \zeta^2(2u_j \phi i - \phi^2)}, \quad (4.14)$$

where

$$u_1 = \frac{1}{2}, \quad u_2 = -\frac{1}{2}, \quad a = \kappa\theta, \quad b = \kappa. \quad (4.15)$$

Here, we take $t = 0$, $S = S_0$, and $v = v_0$. From the above formulas (4.6) and (4.8), we obtain the call prices under the two models, and using Breeden-Litzenberger we could then recover the distribution implied by the call options.

4.2 Carr & Lee method

(a) Strategy of implementation

From Proposition 3.1, we know that a lower bound on the option price is given by the expression

$$-BS(Y_0, Q; \lambda) + \mathbb{E}_0 \lambda(Y_T). \quad (4.16)$$

Here $BS(y, v; f)$ is defined as in (3.2), and in order to maximise the lower Carr & Lee bound we will use λ as in (3.7). The method we will use to find the Carr & Lee lower bound is summarised in Algorithm 1. In the first step of Algorithm 1, we determine the dimensionless implied volatility. In order to do this, we numerically find the zero of the function

$$g(x) = BS(S_0, x; \operatorname{van}_K) - \mathbb{E}_0 [\operatorname{van}_K(S_T)]. \quad (4.17)$$

Recall that the function BS is increasing in its second argument, and that the solution is unique. Using the $I_0(K, T)$, we are able to determine the domain of integration for the optimal λ in (3.7), and with this λ we will be able to compute the lower bound.

Algorithm 1: Procedure for Carr & Lee lower bound

Data: European vanilla options, implied distribution

Result: Lower bound on price of variance call using method from Carr & Lee [7].

- 1 For each available strike K , find $I_0(K, T)$ such that $BS(S_0, I_0(K, T); \text{van}_K) = \text{van}_K$ holds
 - 2 Determine $\lambda(y)$ using the $I_0(K, T)$ from the previous step
 - 3 Evaluate $-BS(S_0, Q; \lambda)$
 - 4 Estimate $\mathbb{E}\lambda(S_T)$ using the implied distribution for S_T
 - 5 Find the lower bound as $-BS(S_0, Q; \lambda) + \mathbb{E}\lambda(S_T)$
-

For the Carr & Lee upper bound, we will implement the functions described in Propositions 3.2 and apply the method in Algorithm 2. The implementation of L is straightforward, and for BP we will numerically estimate the complex integral in (3.18). As stated in Section 3.1, there is room for optimisation in our choice of b_d and b_u , and our choices of b_d and b_u are not necessarily those that yield the lowest possible upper bound for the Carr & Lee method.

Algorithm 2: Procedure for Carr & Lee upper bound

Data: European vanilla options, implied distribution

Result: Upper bound on price of variance call using method from Carr & Lee [7].

- 1 Select appropriate values for b_d, b_u such that $0 < b_d \leq S_0 \leq b_u < \infty$
 - 2 Evaluate $-L^*(S_0; b_d, b_u, Q)$
 - 3 Estimate $\mathbb{E}L^*(S_T; b_d, b_u, Q)$ using the implied distribution for S_T
 - 4 Find the upper bound as $-L^*(S_0; b_d, b_u, Q) + \mathbb{E}L^*(S_T; b_d, b_u, Q)$
-

(b) Numerical results

The numerically determined dimensionless implied volatilities are displayed in Figures 4.3a and 4.3b for the Black-Scholes and Heston models, respectively.

First, consider the dimensionless implied volatility for Black-Scholes. From theory, we expect in this case constant $I_0(K, T) = \sigma^2 T$, which would be 0.08 for our parameter values. Indeed, this is what we observe for mid-range to high strikes. For smaller strikes, however, we see a spike in the dimensionless implied volatility. This appears to be caused by limitations stemming from the accuracy of the solver for $I_0(K, T)$, combined various numerical errors arising from e.g. our discretisation of the target distribution. Note that van_K is defined using OTM options, so for small K we have call options that are far out of the money. The option price, appearing as the term $-\mathbb{E}_0[\text{van}_K(S_T)]$ in (4.17), is thus very close to zero, and the consequences of numerical errors and limited machine precision become noticeable. Nevertheless, it is worth noting that although we see dramatic deviations in the dimensionless implied volatility for small strikes, these do not seem to significantly impact neither the value of $BS(S_0, I_0(K, T); \text{van}_K)$ nor the resulting λ , though this is something that could be further investigated in future works.

Similarly, we also see spikes in the dimensionless implied volatility for the Heston model for small strikes, for the same reasons as discussed above. For mid-range and high strikes

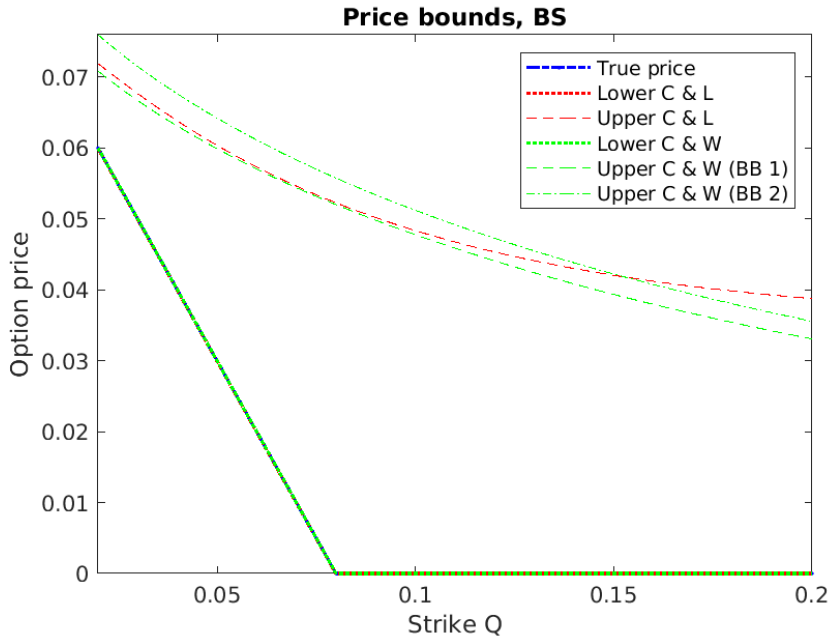


Figure 4.1: *Bounds on the no-arbitrage price for the Black-Scholes variance call. The lower bounds from Carr & Lee (“C & L”) and Cox & Wang (“C & W”) coincide with the true price. The upper bound “BB 1” is when we use the BB construction from the first time step, and “BB 2” from the second timestep.*

the implied volatility is no longer constant as for the Black-Scholes model, but we instead see the characteristic “volatility smile”.

The main interest of this section are the price bounds obtained for the variance calls, and these are displayed together with the “true prices” in Figures 4.1 and 4.2 for the Black-Scholes and Heston models respectively.

For the bounds in the Black-Scholes case, our numerical results agree with our theoretical observation that for log-normal target distributions, the subhedging strategy perfectly replicates the variance call and the lower bound coincides with the true price of the option. In comparison, the upper bound is further away from the true price, though it is possible that we can decrease the upper bound by improving our choice of parameters b_d , b_u . Optimisation of the parameters, so that the upper bound is minimised, could also be investigated in future works.

For the Heston bounds on the other hand, there is now a gap between each bound and the “true price”. The lower bound still appears to be closer to the true price than the upper one, agreeing with the observations of Carr & Lee [7], but once again it is possible that the upper bound can be further reduced. The shape of the lower bound is now smoother and more curved than in the Black-Scholes case, which can be motivated by the fact that we now see a non-atomic distribution of implied volatilities and realised variances.

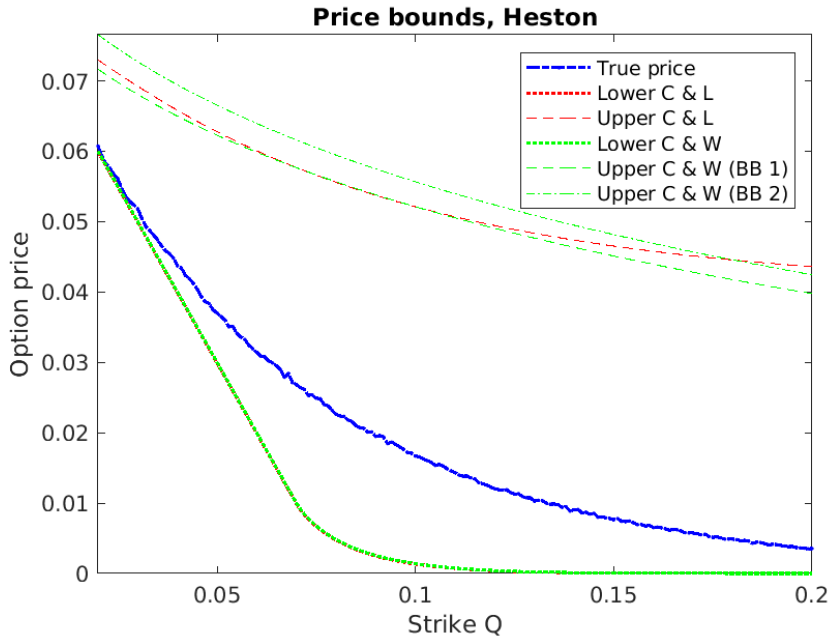


Figure 4.2: Bounds on the no-arbitrage price for the Heston variance call. The lower bounds from Carr & Lee (“C & L”) and Cox & Wang (“C & W”) almost coincide. The upper bound “BB 1” is when we use the BB construction from the first time step, and “BB 2” from the second timestep.

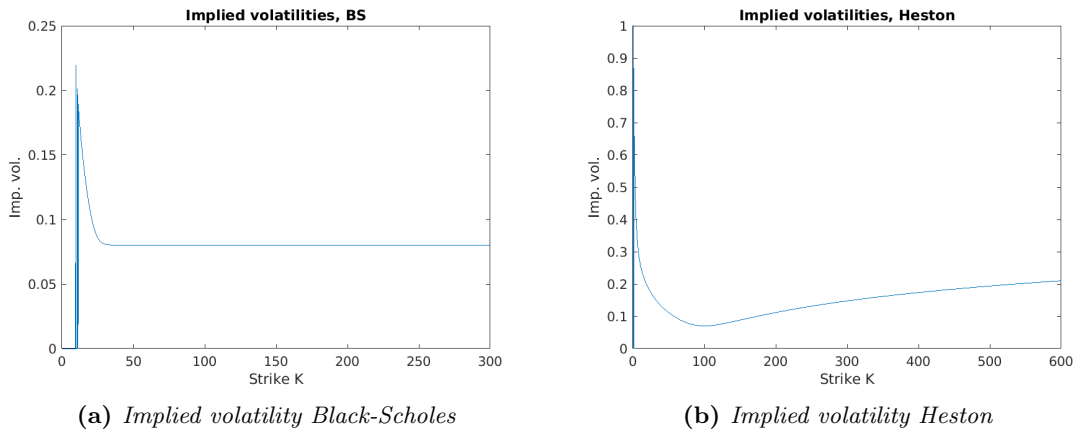


Figure 4.3: Dimensionless implied volatilities for (a) the Black-Scholes data, and (b) the Heston data.

4.3 Cox & Wang method

A summary of the method that we employ for the Cox & Wang approach is given in Algorithm 3. The general method of implementation will be similar for the lower and upper bounds, and will differ primarily in what free boundary problem we solve in the second step.

For the first step of Algorithm 3, we need to determine the potentials U_ν and U_μ of the initial and target distributions, which we need to properly frame the free boundary problems. For our purposes, we will have initial distribution $\nu \sim \delta_{S_0}$, and μ the (implied)

target distribution. Recall Definition 2.5, and that generally we would need to evaluate an integral to determine the potentials. In our implementation, however, we will exploit some useful properties of the distributions at hand to reduce the computational cost of determining the potentials. Firstly, for the initial distribution $\nu = \delta_{S_0}$ we directly get the potential

$$U_\nu(x) = - \int_{\mathbb{R}} |y - x| \delta(y - S_0) dy = -|x - S_0|. \quad (4.18)$$

Secondly, for the potential U_μ of the target distribution, we can use the Breeden-Litzenberger formula as in Cox & Wang [13] to obtain the expression

$$U_\mu = S_0 - 2C_0(x) - x. \quad (4.19)$$

The simple formulas (4.18) and (4.19) will allow us to directly determine the potentials and avoid numerical integration, significantly improving the performance of our implementation. The remaining steps of Algorithm 3 will be explained in greater detail below.

Algorithm 3: Procedure for Cox & Wang bounds

Data: European vanilla options, implied distribution

Result: Price bounds on variance call using Root or Rost embeddings.

- 1 Determine potentials U_ν and U_μ
 - 2 Find solution u to free boundary problem (3.23) (Root) or (3.32) (Rost)
 - 3 Find barrier function R (Root) or \bar{R} (Rost) using u from previous step
 - 4 Simulate paths of Z hitting the barrier to obtain distribution of hitting times
 - 5 Use distribution of hitting times to determine $\mathbb{E}(\tau - Q)^+$
-

(a) Implementation of Root embedding

For the Root embedding, we will solve the free boundary problem (3.23), as formulated in Gassiat et al. [28]. Recall that we will be able to characterise the Root barrier through the solution to the following problem:

$$\begin{cases} \min(u - U_\mu, \partial_t u - \frac{\sigma(x)^2}{2} \partial_{xx} u) = 0, & \text{on } (0, \infty) \times \mathbb{R}, \\ u(0, x) = U_\nu(x), \\ u(\infty, x) = U_\mu(x). \end{cases} \quad (4.20)$$

We want to discretise the above problem using an explicit finite difference scheme.

Approximate the target distribution as being supported on some bounded interval $[S_{min}, S_{max}]$. Introduce a mesh with time step $\Delta t := T/M$ and spatial step $\Delta x := (S_{max} - S_{min})/(N - 1)$, where M is the number of steps taken in time in the scheme and N the number of grid points in the spatial dimension. Let $t_m := m\Delta t$ for $m \in \{0, 1, \dots, M\}$, and $x_1 := S_{min}$, $x_N := S_{max}$, with interior grid points $x_n = S_{min} + (n - 1)\Delta x$ for $n \in \{2, 3, \dots, N - 1\}$. Let u_n^m be the approximation of the value $u(t_m, x_n)$ in the discretisation. We then take the initial condition

$$u_n^0 = U_\nu(x_n), \quad n \in \{1, 2, \dots, N\} \quad (4.21)$$

and the boundary conditions

$$u_1^m = U_\nu(x_1), \quad u_N^m = U_\nu(x_N). \quad (4.22)$$

Discretising the heat equation above using an explicit scheme, we obtain the expression

$$\frac{u_n^{m+1} - u_n^m}{\Delta t} = \frac{x_n^2}{2} \frac{u_{n+1}^m - 2u_n^m + u_{n-1}^m}{(\Delta x)^2}. \quad (4.23)$$

Thus, to find our (discretised) solution, we iterate forward in time by taking

$$u_n^{m+1} = \max [U_\mu(x_n), u_n^m + \lambda x_n^2 (u_{n+1}^m - 2u_n^m + u_{n-1}^m)], \quad (4.24)$$

where $\lambda = \Delta t / (2(\Delta x)^2)$. By Proposition 1 in Gassiat et al. [28], our discretised solution will converge to the true solution in the L^∞ -norm as our mesh size goes to zero, provided that the Courant-Friedrichs-Lewy (CFL) condition $\Delta t |\sigma|_{\infty; [S_{min}, S_{max}] \times [0, T]} = \Delta t S_{max} < (\Delta x)^2$ holds and that the assumptions on ν , μ , and σ in Theorem 3.3 hold. We can choose Δt and Δx such that the CFL conditions holds, and since our target distribution is supported on \mathbb{R}_+ , local ellipticity also holds. Hence, we may use the above explicit scheme to find a discretisation of the solution u of the free boundary problem (4.20), and this concludes the second step of Algorithm 3.

We know that $u(t, x) = U_\mu(x)$ holds in the Root barrier, and so once we have solved the above problem we take the barrier function to be $R(x_n) = \min\{t_m; u_n^m = U_\mu(x_n)\}$, as is the third step of Algorithm 3. Note that this is a discretised version of the barrier, and we approximate the continuous barrier using cubic spline interpolation.

Knowing the barrier function, we are ready for the fourth step of Algorithm 3, where we sample from the distribution of Root stopping times using Monte Carlo methods. The obtained barrier should be such that if we start a geometric Brownian motion $dZ_t = Z_t dW_t$ at $Z_0 = S_0$ and stop it when it hits the barrier, the stopped values should have the same law as that of the target distribution, and the hitting times will be the Root stopping times. Hence, comparing the distribution of the stopped values to the target distribution allows us to verify that the hitting times indeed do embed the target distribution in the geometric Brownian motion, and that they thus are in $SEP(Z, \mu)$.

The fifth and final step of Algorithm 3 is to use the distribution of the Root stopping times resulting from our Monte Carlo path simulations to estimate the optimal lower bound $\mathbb{E}[(\tau_R - Q)^+]$ on the no-arbitrage price for the variance call.

(b) Implementation of Rost embedding

Our implementation of the Rost embedding follows largely the same structure as for the Root embedding, except that we are now solving the free boundary problem

$$\begin{cases} \partial_t u = \min \left(0, \frac{\sigma(x)^2}{2} \partial_{xx} u \right) & \text{on } (0, \infty) \times \mathbb{R}, \\ u(0, x) = U_\nu(x) - U_\mu(x). \end{cases} \quad (4.25)$$

We discretise the problem in a similar fashion as above, approximating the support of the target distribution by a bounded interval and using a similar mesh as before. This time, our initial condition instead reads

$$u_n^0 = U_\nu(x_n) - U_\mu(x_n), \quad n \in \{1, 2, \dots, N\} \quad (4.26)$$

and we impose the boundary conditions

$$u_1^m = U_\nu(x_1) - U_\mu(x_1), \quad u_N^m = U_\nu(x_N) - U_\mu(x_N). \quad (4.27)$$

Furthermore, we use an explicit finite difference scheme to discretise the PDE as

$$\frac{u_n^{m+1} - u_n^m}{\Delta t} = \min \left(0, \frac{x_n^2}{2} \frac{u_{n+1}^m - 2u_n^m + u_{n-1}^m}{(\Delta x)^2} \right), \quad (4.28)$$

and by solving for u_n^{m+1} we get (with $\lambda = \Delta t / (2(\Delta x)^2)$ as before)

$$u_n^{m+1} = u_n^m + \min \left(0, \lambda x_n^2 (u_{n+1}^m - 2u_n^m + u_{n-1}^m) \right). \quad (4.29)$$

We then step forward in time using the above scheme and thus obtain a discretisation u_n^m of $u(x, t)$.

In analogy with the Root case, we will be able to determine the Rost barrier from the solution to the free boundary problem (4.25). We know that $u(x, t) = u(x, 0) = U_\nu(x) - U_\mu(x)$ holds in the Rost barrier $\bar{\mathcal{B}}$, and so we determine the Rost barrier function by $\bar{R}(x_n) = \max\{t_m; u_n^m = U_\nu(x_n) - U_\mu(x_n)\}$, and then use cubic spline interpolation for any x between the grid points.

Once we have determined the Rost barrier, we should in principle proceed in the same fashion as we did for the Root embedding, by simulating path hits and determining the distribution of the Rost hitting times. However, this proves to be a more difficult task than for the Root barrier, due to the delicate asymptotic character of the barrier around the initial value S_0 . To embed values in a neighbourhood of S_0 , the Rost barrier will have to stop paths at times close zero where the barrier function is very steep. In this region, small errors in the hitting time get amplified to larger errors in the embedded value, and the accuracy of the path can have a significant impact on the results. For these reasons, we extend our methodology for the Rost embedding in an attempt to improve the embedding for small timescales.

Some straightforward ways to improve the asymptotics of the embedding include simply using a finer mesh when solving the free boundary problem (to improve the accuracy of the obtained Rost barrier), and choosing an appropriately short time step for the path simulation.

Another method that could potentially improve the asymptotics is to apply a Brownian bridge construction for the first few time steps. If the size of the time step Δt is very small, then Z is roughly constant over each interval, and so over an interval $[t_n, t_n + \Delta t)$ we could approximate the dynamics of Z over $[t_n, t_n + \Delta t)$ by

$$dZ_t = Z_{t_n} dW_t, \quad (4.30)$$

with Z_{t_n} constant, so that Z behaves like an arithmetic Brownian motion. Over each time step $[t_n, t_{n+1}]$ in the simulated path, we can then condition the value of Z_{θ_n} at any intermediate time $\theta_n \in [t_n, t_{n+1}]$ on the boundary values Z_{t_n} and $Z_{t_{n+1}}$, whereby Z_{θ_n} becomes a Brownian bridge. Using standard theory for Brownian bridges, we can sample from the distribution of the maximum $\widehat{M}_{+,t_n} = \sup_{\theta \in [t_n, t_{n+1}]} Z_\theta$ and the minimum $\widehat{M}_{-,t_n} = \inf_{\theta \in [t_n, t_{n+1}]} Z_\theta$ of Z over this interval by using

$$\widehat{M}_{\pm, t_n} = 0.5 \left(Z_{t_n} + Z_{t_{n+1}} \pm \sqrt{(Z_{t_{n+1}} - Z_{t_n})^2 - 2\Delta t Z_{t_n}^2 \log(U)} \right), \quad (4.31)$$

where $U \sim \mathcal{U}([0, 1])$ (see e.g. formula (6.50) in Glasserman [29]). Unlike the case of a barrier option, however, we have a non-constant barrier function. Nonetheless, when using our Brownian bridge construction (here abbreviated as “BB”), we approximate the upper part of the barrier over the interval $[t_n, t_{n+1}]$ as being the (constant) cubic spline interpolated barrier value at the midpoint $(t_n + t_{n+1})/2$. We then compare the sampled maximum value with this constant level, and if the maximum exceeds the barrier, we register a hit (at the midpoint time). We do the same for the minimum and the lower part of the barrier. Using the Brownian bridge theory that we have just outlined, we attempt to improve the numerical accuracy of the Rost embedding for values around S_0 .

(c) Numerical results

The results for the Root embeddings are shown in Figure 4.4 for the Black-Scholes model, and in Figure 4.5 for the Heston model. We used 50,000 paths each with 10,000 time steps for the Root path hitting simulation, and 20,000 paths each with 100,000 time steps for the Rost path hitting.

For the Root embedding results in the Black-Scholes case, our numerical results agree well with what we expected from theory. In Figure 4.4a, we see that the numerically determined Root barrier is indeed a constant, save for some slight curvature at very high strikes due to limitations in numerical precision. In particular $R(x) = \sigma^2 T = 0.08$, so that all the simulated geometric Brownian paths in Figure 4.4b are stopped at the same time 0.08. As seen in Figure 4.4c, the stopped values follow the log-normal target distribution, and the hitting times in the histogram in Figure 4.4d can be viewed as having (approximately) a distribution of $\delta(x - \sigma^2 T)$. Furthermore, the lower bound in this case coincides with the “true price”, as seen in Figure 4.1.

For the Heston model that we implemented, the Root barrier is as in Figure 4.5a, which has a less trivial shape than in the Black-Scholes case, and in Figure 4.5b we show simulated geometric Brownian paths hitting the barrier. Once again, the embedding property of the barrier becomes clear in Figure 4.5c, where we see that the stopped values do indeed follow the Heston target distribution, and the distribution of the corresponding Root hitting times is visualised in Figure 4.5d. This non-atomic distribution of stopping times gives rise to a smoother lower bound profile than the piecewise linear $(\sigma^2 T - Q)^+$, as seen in Figure 4.2.

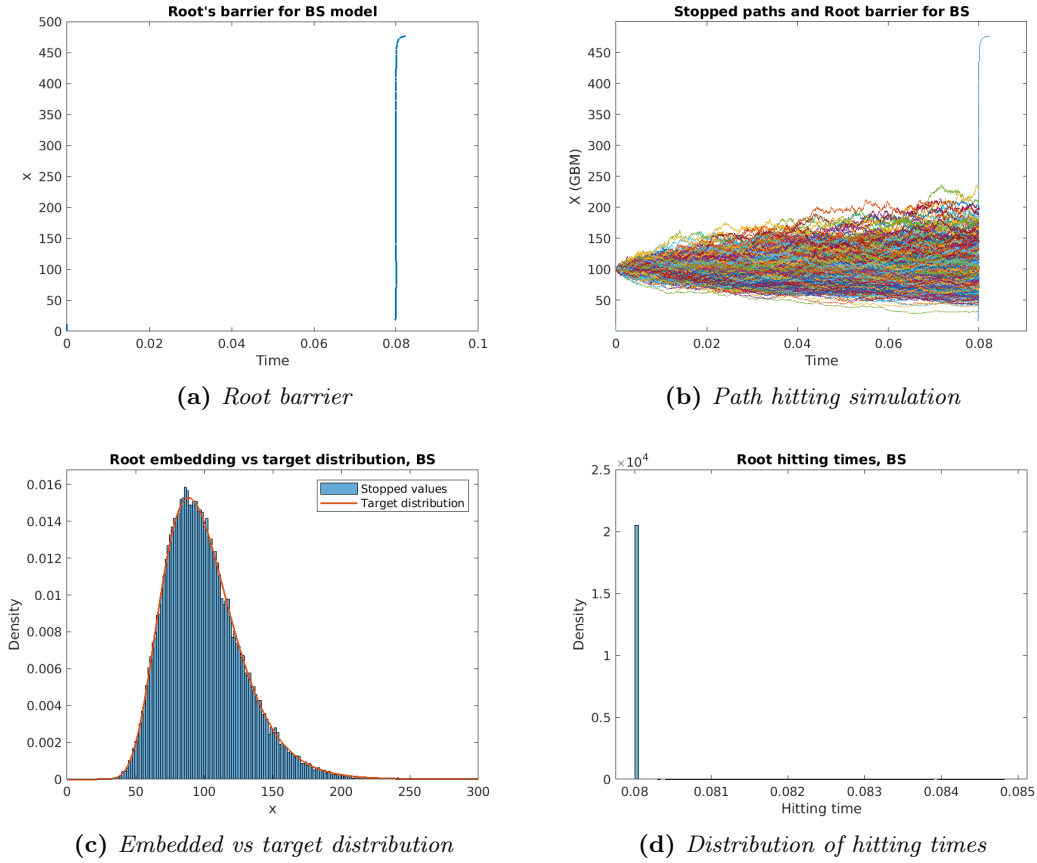


Figure 4.4: *Root embedding for the data from the Black-Scholes model.*

Moving on to the results for the Rost embedding, the Rost barriers together with simulated paths are shown in Figure 4.6a for the Black-Scholes model and in Figure 4.7a for the Heston model. Unlike the case for the Root barriers above, both models now have non-trivial barrier functions, and we see that the magnitude of the slope of the barrier becomes very large as we approach S_0 .

Simply simulating path hitting without any Brownian bridge constructions gives a distribution of stopped values as in Figure 4.6b for Black-Scholes and in Figure 4.7b for Heston. We here clearly see the problems with embedding values in a neighbourhood of the initial value. There is a clear gap around S_0 for both models, which is a sign that not enough stopping happens at earlier times, since paths that should have stopped at values close to zero now survive and hit the barrier at later times.

Due to the fact that the obtained hitting times do not in fact embed the target distributions (Black-Scholes and Heston respectively) in the geometric Brownian motion, we do not trust the reliability of the distribution of the hitting times for finding price bounds. Thus, we are motivated to attempt to improve the accuracy of our embedding by using the Brownian bridge construction described above. We apply sampling of the maximum and minimum for the first 30 time steps of each path, working backwards in time in order to successively update the first hitting time for each path. Note that this process may only decrease the first hitting time, and thus by the monotonicity of the upper and lower halves

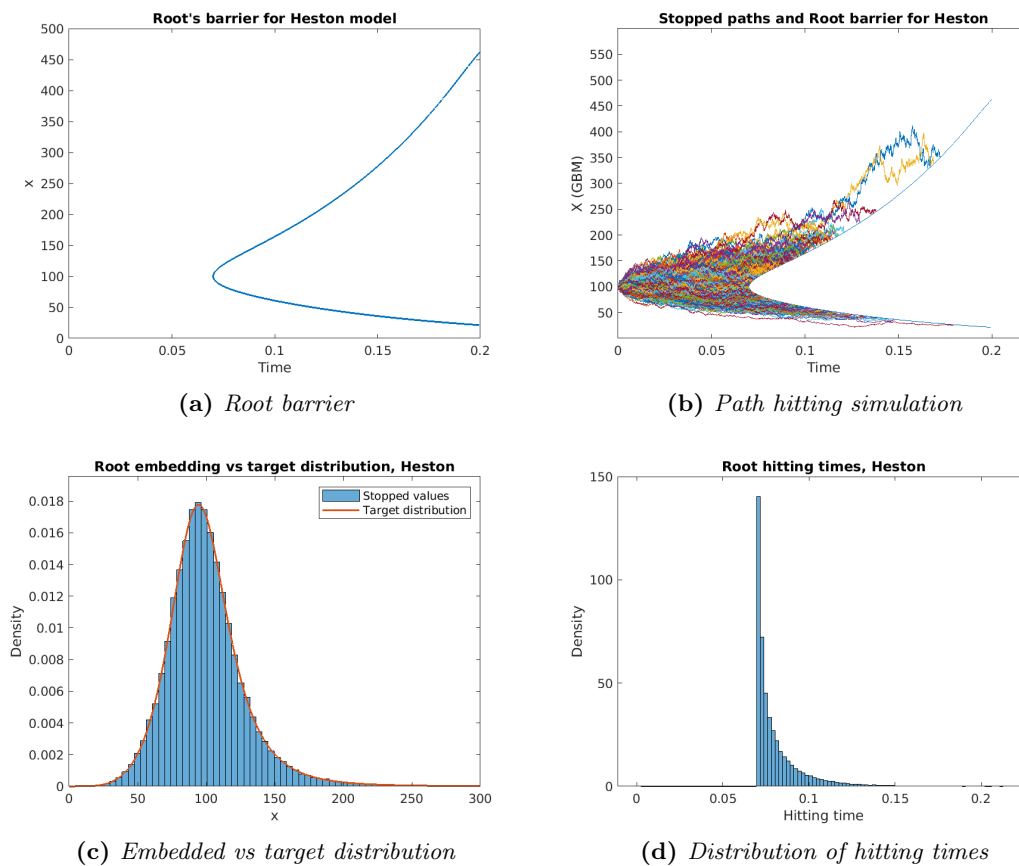


Figure 4.5: *Root embedding for the data from the Heston model.*

of the barrier respectively, it can only move the stopped value for each path closer to S_0 .

The resulting distributions of the stopped values when using the Brownian bridge construction for the first 30 time steps are shown in Figures 4.6c for Black-Scholes and 4.7c for the Heston model. We see that the gap indeed gets closed, and instead we rather get spikes at S_0 surrounded on both sides by slightly lower densities than the target distribution. It is possible that our Brownian bridge construction is overcompensating the early stopping. One plausible explanation for this phenomenon is that our assumption that we may approximate the barrier by a constant over each interval is too strong, especially in the first time step where the barrier has a very steep slope. For this reason, we decided to also try implementing the Brownian bridge construction backwards in time only to the second time step, so that we do not sample the maximum and minimum in the very first interval. This instead yielded the embeddings in Figure 4.6d and 4.7d for Black-Scholes and Heston respectively. We now see that although the gap appears to be not as closed as before (especially for the Black-Scholes case), the spikes at S_0 become less pronounced.

4.4 Comparison of numerical results

The first and most fundamental property that we verify from the Figures 4.1 and 4.2 is that for both approaches, the bounds do enclose the true price of the variance call. If

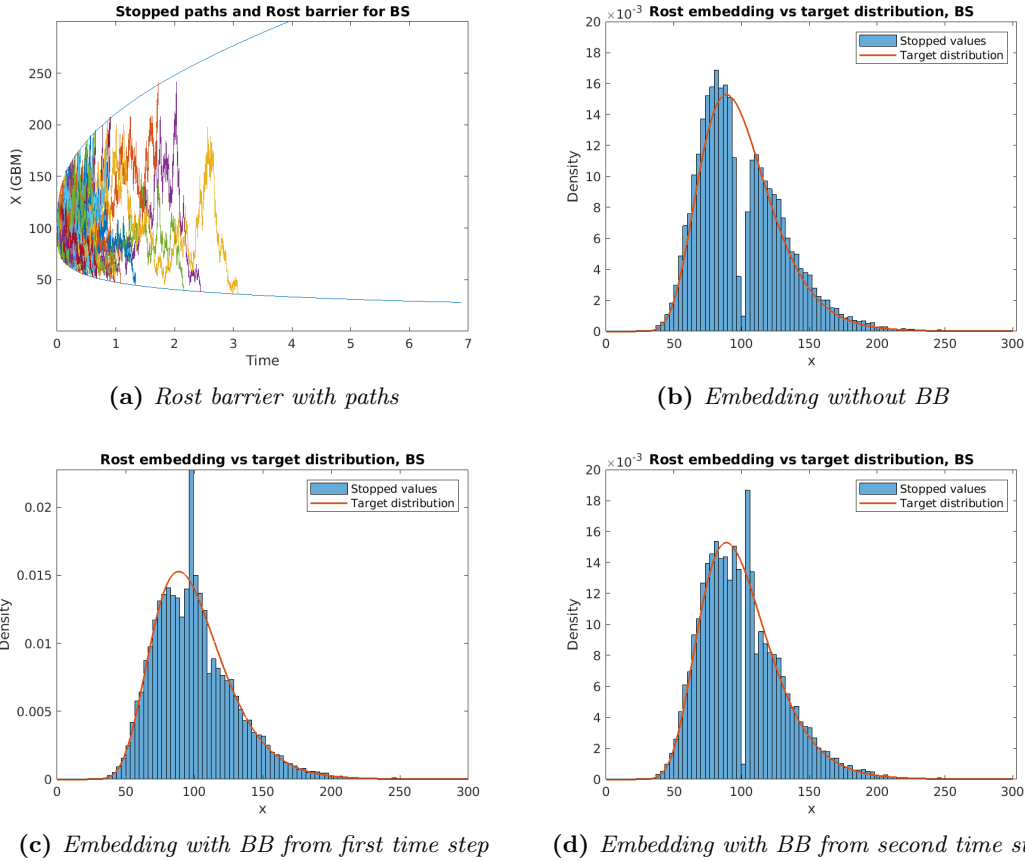


Figure 4.6: Rost embedding results for the data from the BS model for different uses of our Brownian bridge construction (BB).

we have accurately determined the distribution of the Root and Rost stopping times for the Black-Scholes and Heston models, then the Cox & Wang bound profiles that we have obtained should be the optimal lower and upper bounds for the variance calls in each case. More explicitly, the Cox & Wang lower bound should always be above the Carr & Lee lower bound (possibly attaining equality), and vice versa for the Cox & Wang upper bound being below the Carr & Lee upper bound.

This property indeed holds for the lower bounds in both the Black-Scholes and Heston cases, where the lower bounds are equal for Black-Scholes, and the Cox & Wang bound is marginally higher than the Carr & Lee bound for Heston. This confirms the findings of Carr & Lee [7], where they compared their lower bound to the Root bound for a Heston model calibrated using the same parameters as we used (albeit they used a time horizon of $T = 1$ instead of $T = 2$ as we did). In both the Black-Scholes and Heston cases, the Carr & Lee lower bounds are extremely close to the Cox & Wang lower bounds, meaning that at least for the models that we have tested here, the Carr & Lee method provides a useful approximation of the optimal lower bound on the no-arbitrage price of the variance calls.

For the upper bounds on the other hand, we find that only when using Brownian bridge from the first step onward does the Cox & Wang upper bound actually lie below the Carr & Lee upper bound. When omitting the first interval from the Brownian bridge construction,

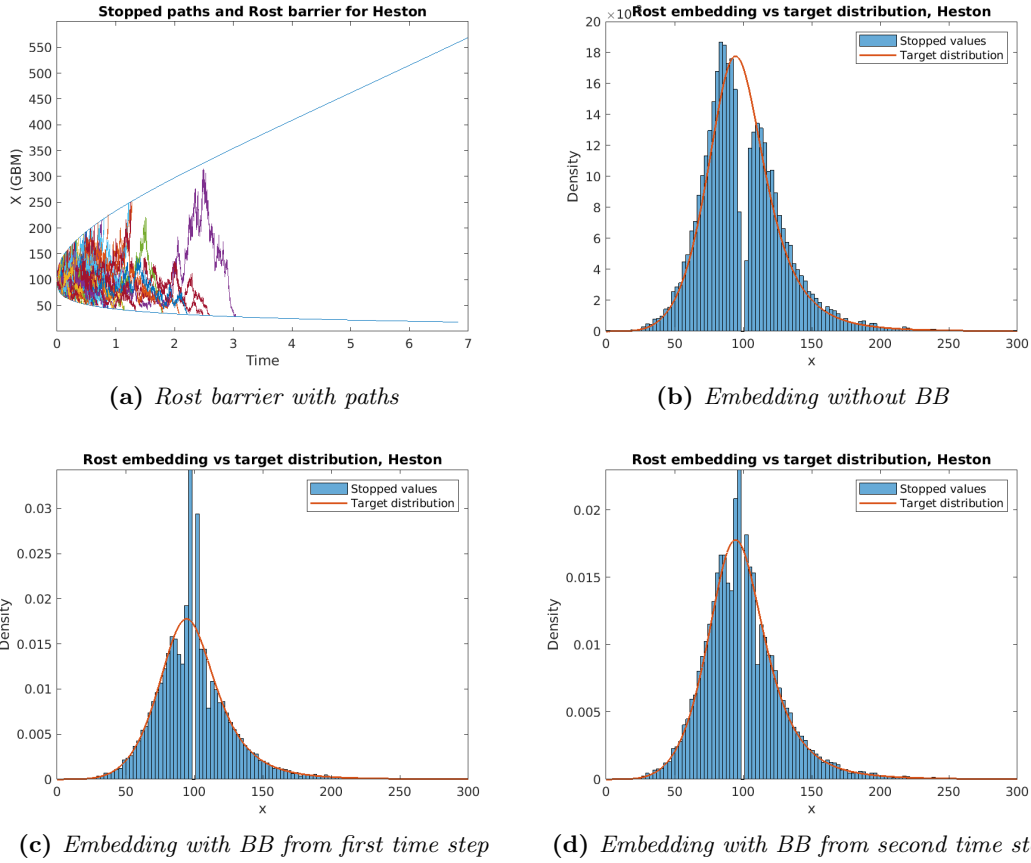


Figure 4.7: Rost embedding results for the data from the Heston model for different uses of our Brownian bridge construction (BB).

the Cox & Wang upper bound exceeds that of Carr & Lee. An immediate explanation for why we expect the upper bound to be lower in the case when we include the first time step in the Brownian bridge construction than in the case when we start from the second time step onward is that as we stop some paths earlier, the distribution of the stopping times will shift to the left, in the sense that probability mass will be transported to smaller times. This in turns causes the quantity $\mathbb{E}(\tau_{\bar{R}} - Q)^+$ to be lower for all Q , and we thus obtain a decrease in the bound.

Assuming that the Carr & Lee upper bounds that we have obtained are in fact valid, the Cox & Wang upper bounds when we start the Brownian bridge from the second time step are obviously suboptimal, and they may be rejected. The Cox & Wang upper bounds when we include the first time step in the Brownian bridge construction do satisfy the condition that they lie below the Carr & Lee upper bounds, but note that this is only a necessary condition for optimality and not a sufficient one. Since the distributions of the stopped values in the Rost case still deviate noticeably from the target distribution even after our applying our Brownian bridge method, we are not confident that we have accurately determined the distribution of the Rost stopping times. An interesting observation is that when looking at the (unadjusted) distributions of the stopped values, there seems to be a larger increase in the density for values below S_0 than for those above. This could be related to the fact that

the Rost barriers for both Black-Scholes and Heston display a higher curvature for values just below S_0 than for values just above, and that this affects the impact of interpolation errors and similar on the embedding for values smaller than S_0 . It is also possible that this is explained by the fact that the density itself is the highest below S_0 , and that the lack of embedding around S_0 simply scales up the remaining density roughly equally.

For both models tested here, the true price is generally closer to the lower bound than the upper bound, which agrees with the observations in Carr & Lee [7]. In the Heston case we see that for very small strikes the true price almost coincides with the lower bound from the Carr & Lee approach, and that they seem to approach each other asymptotically in the limit $Q \rightarrow 0$. This is reasonable, and has an intuitive explanation. The Carr & Lee subhedging strategy is closely related to the strategy replicating a variance swap, where slight modifications are made to further increase the lower bound on the variance call. In the limit $Q \rightarrow 0$, we have both that the variance call will behave as a variance swap, and that the domain of integration in (3.7) will approach \mathbb{R}_+ , so that we recover the strategy replicating a variance swap. Thus, asymptotically, the Carr & Lee subhedging strategy will replicate the variance call as the strike goes to zero, and the lower bound approaches the true price.

In our implementation of the Carr & Lee approach, we need to numerically evaluate an integral for each strike, which can be costly for high accuracies. For Cox & Wang on the other hand, once we know the distribution of the hitting times, we can quickly determine bounds for a very large number of strikes. Overall though, our Cox & Wang implementation is more computationally demanding due to the necessity of high accuracy both when solving the free boundary boundary problem and when simulating the path hits.

We would like to conclude our discussion here by mentioning some possible areas of improvement and further investigation. Our methodology for determining the Rost bound could be improved to ensure that we properly embed the target distribution. In addition to our Brownian bridge construction, it is possible to e.g. use adaptive mesh refinement. This allows for a much finer mesh size around S_0 , so that the computational effort is directed to the critical region.

Another area that could be further explored is the behaviour at very small strikes, where the precision of the numerics can significantly affect e.g. the implied volatilities obtained. In a practical sense however, and based on our above arguments about the asymptotics as $Q \rightarrow 0$, it could also be possible to approximate the variance call by a variance swap for extremely small strikes, and it is not clear how relevant calls at such small strikes are in practice.

Moreover, it would be interesting to test the two approaches on actual market data to see how well our findings for the Black-Scholes and Heston models extend to the real world setting, although extra care would need to be taken to deal with some of the idealised assumptions made here, e.g. the fact that we do not longer have a continuum of strikes

available. For some results on the effects when only a finite number of strikes is traded, see e.g. Bühler [5], Davis & Hobson [18], Cousot [11], and Davis et al. [17].

Optimisation of the parameters b_d , b_u in the Carr & Lee superhedging can also be investigated, although in both our findings and those of Carr & Lee [7], the upper Carr & Lee bound appears relatively close to the Rost bound.

Chapter 5. Conclusions

We have compared the approaches by Carr & Lee [7] and Cox & Wang [12,13] for bounding the no-arbitrage price of variance calls. We did this first from a theoretical viewpoint, and especially in the light of Remark 5.4 in Cox & Wang [13] for the connection between the subhedging strategies of the two approaches. This was followed by numerical implementation of the approaches, and their performance was tested on simulated data.

We showed Proposition 3.8 that the Carr & Lee subhedging strategy perfectly replicates variance calls when the price process is a martingale with a log-normal target distribution. Furthermore, when using a constant barrier function instead of the Root barrier function in the Cox & Wang subhedging strategy, we proved Theorem 3.9 that the strategy reduces to Carr & Lee subhedging. This confirms and motivates Remark 5.4 made in Cox & Wang [13].

Furthermore, for the numerical implementation we confirmed the expectations from theory that both the Carr & Lee and Cox & Wang lower bounds coincide with the true price in the case of the Black-Scholes model. Moreover, the Carr & Lee lower bound was very close to that of Cox & Wang also for the Heston model we implemented. This suggests that Carr & Lee subhedging could be a useful and straightforward approximation of the optimal robust subhedging strategy by Cox & Wang, especially for practitioners due to its relatively simple hedging strategy and for its less computationally demanding method of determining price bounds. The upper bounds proved to be more difficult to determine in the Cox & Wang case, where the asymptotic character of the Rost barrier made simulation of path hitting even more challenging. Simply simulating paths and registering barrier hits did not result in a proper embedding of the target distribution, and so we tried improving our results by using a Brownian bridge construction. Although this did improve the embedding, we believe that there is still room for further improvements.

Possible areas of future work include testing the approaches on real-world data, improving the Rost embedding (e.g. by using adaptive mesh refinement when determining the barrier), optimising the parameters for the Carr & Lee superhedging to lower the upper bound, and investigating how limitations on the numerical precision affect the results in the domain of very small and very large strikes.

Bibliography

- [1] Hansjörg Albrecher, Philipp Arnold Mayer, Wim Schoutens, and Jurgen Tistaert. The little Heston trap. *Wilmott*, 1:83–92, 2007.
- [2] Fischer Black and Myron Scholes. The pricing of options and corporate liabilities. *Journal of Political Economy*, 81(3):637–654, 1973.
- [3] Oleg Bondarenko. Variance trading and market price of variance risk. *Journal of Econometrics*, 180(1):81 – 97, 2014.
- [4] Douglas T. Breeden and Robert H. Litzenberger. Prices of state-contingent claims implicit in option prices. *The Journal of Business*, 51(4):621–651, 1978.
- [5] Hans Bühler. Expensive martingales. *Quantitative Finance*, 6(3):207–218, 2006.
- [6] Peter Carr and Roger Lee. Volatility derivatives. *Annual Review of Financial Economics*, 1(1):319–339, 2009.
- [7] Peter Carr and Roger Lee. Hedging variance options on continuous semimartingales. *Finance and Stochastics*, 14(2):179–207, 04 2010.
- [8] Peter Carr and Dilip Madan. Towards a theory of volatility trading. In *Option Pricing, Interest Rates, and Risk Management*, pages 417–427. University Press, 1998.
- [9] Peter P. Carr and Roger Lee. Robust Replication of Volatility Derivatives. *SSRN Electronic Journal*, 2008.
- [10] Rene M. Chacon. *Barrier Stopping Times and the Filling Scheme*. PhD thesis, University of Washington, 1985.
- [11] Laurent Cousot. Conditions on option prices for absence of arbitrage and exact calibration. *Journal of Banking & Finance*, 31(11):3377 – 3397, 2007.
- [12] Alexander M. G. Cox and Jiajie Wang. Optimal robust bounds for variance options. *arXiv:1308.4363 [math, q-fin]*, August 2013. arXiv: 1308.4363.
- [13] Alexander M. G. Cox and Jiajie Wang. Root’s barrier: Construction, optimality and applications to variance options. *The Annals of Applied Probability*, 23(3):859–894, 2013.

- [14] John C. Cox, Jonathan E. Ingersoll, and Stephen A. Ross. A theory of the term structure of interest rates. *Econometrica*, 53(2):385–407, 1985.
- [15] John C. Cox and Stephen A. Ross. The valuation of options for alternative stochastic processes. *Journal of Financial Economics*, 3(1):145–166, January 1976.
- [16] K. Dambis. On the decomposition of continuous submartingales. *Theory of Probability & Its Applications*, 10(3):401–410, 1965.
- [17] Mark Davis, Jan Obłój, and Vimal Raval. Arbitrage bounds for prices of weighted variance swaps. *Mathematical Finance*, 24(4):821 – 854, 2014.
- [18] Mark H. A. Davis and David G. Hobson. The range of traded option prices. *Mathematical Finance*, 17(1):1–14, 2007.
- [19] Kresimir Demeterfi, Emaunuel Derman, Michael Kamal, and Joseph Zou. A guide to volatility and variance swaps. *Journal of Derivatives*, 6(4):9–32, Summer 1999.
- [20] Emanuel Derman and Iraj Kani. Riding on a smile. *Risk*, 7, 01 1994.
- [21] Hermann Dinges. Stopping sequences. *Séminaire de probabilités de Strasbourg*, 8:27–36, 1974.
- [22] Adrian A. Drăgulescu and Victor M Yakovenko. Probability distribution of returns in the Heston model with stochastic volatility. *Quantitative Finance*, 2(6):443–453, 2002.
- [23] Lester E. Dubins and Gideon Schwarz. On continuous martingales. *Proceedings of the National Academy of Sciences of the United States of America*, 53(5):913–916, 1965.
- [24] Bruno Dupire. Arbitrage pricing with stochastic volatility. Société Générale, 1993.
- [25] Bruno Dupire. Pricing with a smile. *Risk*, 7:18–20, 01 1994.
- [26] Bruno Dupire. Volatility derivatives modelling. Bloomberg LP, 2005. Cited through Carr & Lee, “Hedging variance options on continuous semimartingales” (2010), original work by Dupire appears no longer accessible.
- [27] Bruno Dupire. Arbitrage bounds for volatility derivatives as a free boundary problem. https://www.math.kth.se/pde_finance/presentations/Bruno.pdf, 2005-08-16. Presentation given for “PDE and Mathematical Finance” at KTH, Stockholm.
- [28] Paul Gassiat, Harald Oberhauser, and Gonçalo dos Reis. Roots barrier, viscosity solutions of obstacle problems and reflected FBSDEs. *Stochastic Processes and their Applications*, 125(12):4601 – 4631, 2015.
- [29] Paul Glasserman. *Monte Carlo methods in financial engineering*. Applications of mathematics. Springer, New York, 2004.

- [30] Julien Guyon and Pierre Henry-Labordere. The Smile Calibration Problem Solved. *SSRN Electronic Journal*, 2011.
- [31] Steven Heston. A closed-form solution for options with stochastic volatility with applications to bond and currency options. *Review of Financial Studies*, 6:327–43, 02 1993.
- [32] David Hobson. *The Skorokhod Embedding Problem and Model-Independent Bounds for Option Prices*, pages 267–318. Springer Berlin Heidelberg, Berlin, Heidelberg, 2011.
- [33] David Hobson and Martin Klimmek. Model independent hedging strategies for variance swaps. *Finance and Stochastics*, 16(4):611–649, 2011.
- [34] John Hull and Alan White. The pricing of options on assets with stochastic volatilities. *The Journal of Finance*, 42(2):281–300, 1987.
- [35] Robert Jarrow, Younes Kchia, Martin Larsson, and Philip Protter. Discretely sampled variance and volatility swaps versus their continuous approximations. *Finance and Stochastics*, 17(2):305–324, Apr 2013.
- [36] Geoffrey Lee, Yu Tian, and Zili Zhu. Monte Carlo pricing scheme for a stochastic-local volatility model. *Lecture Notes in Engineering and Computer Science*, 2:934–939, 07 2014.
- [37] Roger Lord, Remmert Koekoek, and Dick van Dijk. A comparison of biased simulation schemes for stochastic volatility models. *Quantitative Finance*, 10(2):177–194, 2010.
- [38] Robert M. Loynes. Stopping times on Brownian motion: Some properties of Root’s construction. *Zeitschrift für Wahrscheinlichkeitstheorie und Verwandte Gebiete*, 16:211–218, 09 1970.
- [39] Robert C. Merton. Theory of rational option pricing. *The Bell Journal of Economics and Management Science*, 4(1):141–183, 1973.
- [40] Itrel Monroe. On embedding right continuous martingales in Brownian motion. *The Annals of Mathematical Statistics*, 43(4):1293–1311, 1972.
- [41] Milan Mrázek and Jan Pospíšil. Calibration and simulation of Heston model. *Open Mathematics*, 15, 05 2017.
- [42] Anthony Neuberger. The log contract. *Journal of Portfolio Management*, 20(2):74, Winter 1994.
- [43] Jan Oblój. The Skorokhod embedding problem and its offspring. *Probab. Surveys*, 1:321–392, 2004.

- [44] Jan Oblój. On some aspects of Skorokhod embedding problem and its applications in mathematical finance. <https://pdfs.semanticscholar.org/ef38/287600a7197aaffb225bbb307a27ee3774b0.pdf>, 2014.
- [45] Philip E. Protter. *Stochastic Integration and Differential Equations*. Stochastic Modelling and Applied Probability. Springer Berlin Heidelberg New York, 2nd edition, version 2.1 edition, 2005.
- [46] D. H. Root. The existence of certain stopping times on Brownian motion. *The Annals of Mathematical Statistics*, 40(2):715–718, 1969.
- [47] Hermann Rost. The stopping distributions of a Markov process. *Inventiones mathematicae*, 14(1):1–16, Mar 1971.
- [48] Hermann Rost. Skorokhod stopping times of minimal variance. *Séminaire de probabilités de Strasbourg*, 10:194–208, 1976.
- [49] Louis O. Scott. Option pricing when the variance changes randomly: Theory, estimation, and an application. *The Journal of Financial and Quantitative Analysis*, 22(4):419–438, 1987.
- [50] Anatoliy V. Skorokhod. *Studies in the theory of random processes*. Addison-Wesley international series in mathematics. Addison-Wesley, Reading, Mass, 1965.
- [51] Dean Teneng. Limitations of the Black-Scholes model. *International Research Journal of Finance and Economics*, pages 99–102, 01 2011.
- [52] Yu Tian, Zili Zhu, Geoffrey Lee, Fima Klebaner, and Kais Hamza. Calibrating and pricing with a stochastic-local volatility model. *Journal of Derivatives*, 22(3):21–39,5, Spring 2015.